Journal of Human Evolution 60 (2011) 711–730

Contents lists available at ScienceDirect

Journal of Human Evolution

journal homepage: www.elsevier.com/locate/jhevol

Evolution of the mandibular third premolar crown in early *Australopithecus*

Lucas K. Delezene*, William H. Kimbel

Institute of Human Origins, School of Human Evolution and Social Change, Arizona State University, Tempe, AZ 85287-2402, USA

ARTICLE INFO

Article history:
Received 28 August 2010
Accepted 8 January 2011

Keywords:
Canine honing complex
Premolar molarisation
Hadar
Laetoli
Kanapoi
Australopithecus afarensis
Australopithecus anamensis

ABSTRACT

The Pliocene hominins *Australopithecus anamensis* and *Australopithecus afarensis* likely represent ancestor-descendent taxa—possibly an anagenetic lineage—and capture significant change in the morphology of the canine and mandibular third premolar (P_3) crowns, dental elements that form the canine honing complex in nonhuman catarrhines. This study focuses on the P_3 crown, highlighting plesiomorphic features in *A. anamensis*. The *A. afarensis* P_3 crown, in contrast, is variable in its expression of apomorphic features that are characteristic of geologically younger hominins. Temporal variation characterizes each taxon as well. The *A. anamensis* P_3 from Allia Bay, Kenya expresses apomorphic character states, shared with *A. afarensis*, which are not seen in the older sample of *A. anamensis* P_3s from Kanapoi, Kenya, while spatiotemporal differences in shape exist within the *A. afarensis* hypodigm. The accumulation of derived features in *A. afarensis* results in an increased level of P_3 molarisation. P_3 molarisation did not evolve concurrent with postcanine megadontia and neither did the appearance of derived aspects of P_3 occlusal form coincide with the loss of canine honing in hominins, which is apparent prior to the origin of the genus *Australopithecus*. *A. afarensis* P_3 variation reveals the independence of shape, size, and occlusal form. The evolution of the P_3 crown in early *Australopithecus* bridges the wide morphological gap that exists between geologically younger hominins on the one hand and extant apes and *Ardipithecus* on the other.

Introduction

Extant great apes have large, sexually dimorphic canine crowns that participate in a functional complex (the canine honing complex) with the mandibular third premolar (P_3). If, as seems well founded, this complex was ancestral for the hominin clade, then hominin canines reduced in size (both absolutely and relative to postcanine tooth size), canine wear became predominantly apical, and the P_3 lost morphological specializations related to canine honing. The dramatic differences between the morphology and function of this complex in hominins and extant apes have been appreciated for some time. For example, in 1956 John Robinson detailed the dental morphology of southern African australopiths (i.e., *Australopithecus africanus* and *Paranthropus robustus*) and was so struck by the wide morphological gap between the canines and P_3s of these ancient hominins and extant apes that, for the hominins, he did not envision an evolutionary transformation from the ape honing complex; he figured the less specialized hominin form to be primitive because, at that time, no hominin fossils captured the reconfiguration of the canine honing complex that is now known to have occurred (Robinson, 1956; see also Kinzey, 1971). In this study, we focus on one element of this complex, the P_3, in the hominins *Australopithecus anamensis* and *Australopithecus afarensis* and their extant African ape outgroups *Gorilla gorilla* and *Pan troglodytes*. *A. anamensis* and *A. afarensis* preserve a numerically large and morphologically variable sample of P_3s that captures, in part, the functional and morphological transformation of the hominin P_3 crown. The evolution of the P_3 crown in these early *Australopithecus* species significantly bridges the morphological gap between extant apes and the more derived hominin condition while revealing the mosaic nature of the changes that occurred.

The P_3 crowns of *P. troglodytes* and *Gorilla gorilla* are functionally similar and share a suite of morphological features that are plesiomorphic for the hominin clade. As in all extant nonhuman catarrhines, the P_3 of *P. troglodytes* and *G. gorilla* has two functional roles; specifically, the tooth functions both as a hone for the maxillary canine and as a masticatory device in occlusion with the maxillary P3 (P^3). In contrast, the distal mandibular premolar, the P_4, has a single function, mastication. Not surprisingly, in these taxa the mandibular premolars are morphologically distinct, which is termed "premolar heteromorphy" (Fig. 1; Greenfield and Washburn, 1992). In both *Pan* and *Gorilla*, the P_3 has a single cusp, the protoconid (Prd), which is tall and centrally placed along the mesiodistal (MD) axis of the crown. Mesiobuccally, there is a rootward extension of enamel that combines with the tall Prd to

* Corresponding author.
E-mail address: lucas.delezene@asu.edu (L.K. Delezene).

0047-2484/$ – see front matter © 2011 Elsevier Ltd. All rights reserved.
doi:10.1016/j.jhevol.2011.01.006

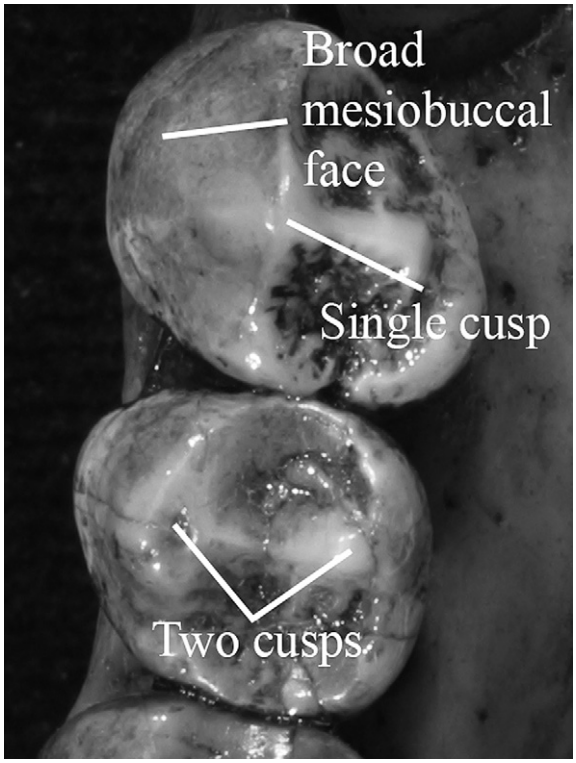

Figure 1. Left P_3 and P_4 of *P. troglodytes*. The mandibular premolars of extant apes are characterized by premolar heteromorphy. The P_3 has a single, tall cusp (protoconid) and a sloping mesiobuccal face that acts as a hone for the maxillary canine; in contrast, the P_4 has two well-developed cusps (protoconid and metaconid) and lacks the honing surface.

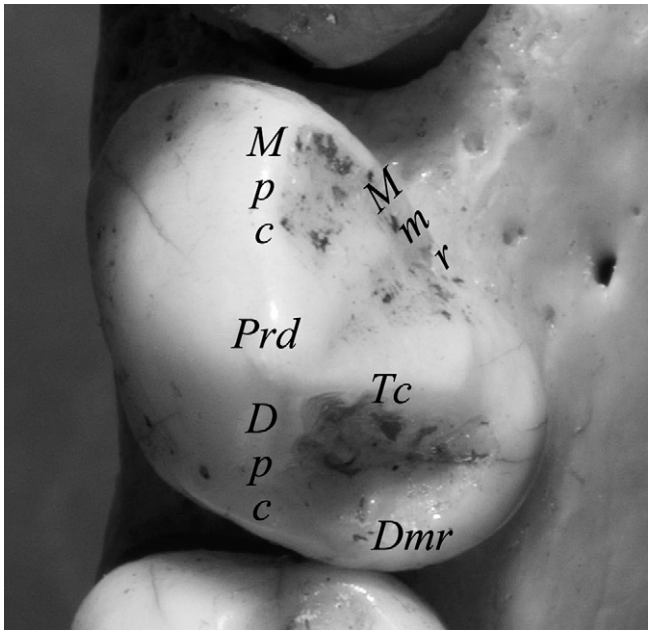

Figure 2. Left P_3 of male *P. troglodytes*. The mesial marginal ridge (Mmr), distal marginal ridge (Dmr), protoconid (Prd), mesial protoconid crest (Mpc), distal protoconid crest (Dpc), and transverse crest (Tc) are labeled. The anterior fovea (Fa) is defined by the Mmr, Mpc, and Tc. The posterior fovea (Fp) is defined by the Dmr, Dpc, and Tc.

form the broad sloping surface that occludes with and hones the maxillary canine. Three crests emanate from the Prd: the mesial protoconid crest (Mpc) extends mesially, the distal protoconid crest (Dpc) extends distally, and the transverse crest (Tc)—referred to as the "transverse ridge" in Leonard and Hegmon (1987)—extends distolingually (Table 1 and Fig. 2; anatomical terms and abbreviations follow Johanson et al. (1982) and Ward et al. (2001)). At the lingual end of the Tc, a small cuspid, an incipient metaconid (Med), is sometimes present and there may be weakly-developed crests that extend mesially and distally from it. In *G. gorilla*, unlike in *P. troglodytes*, the Tc curves distally as it courses towards the distolingual crown margin (Figs. 1–3). The anterior fovea (Fa) is lingual to the Mpc and mesial to the Tc. The mesial marginal ridge (Mmr), which extends from the Mpc to the Tc, is usually absent or poorly developed in *P. troglodytes* and is usually absent in *G. gorilla* (Fig. 4; see also Suwa, 1990). When present, the Mmr is divisible into two segments, the lingual segment of the Mmr begins at the Tc and the buccal segment begins at the Mpc (Suwa, 1990). The two segments of the Mmr run cervically from their respective origins and meet at an acute angle on the mesiolingual surface of the tooth near the cervix. If the Mmr is present, when the tooth is viewed lingually, the sloping Mmr segments combine with a sloping Mpc and Tc to create a diamond-shaped Fa in *P. troglodytes* (Fig. 4). In *G. gorilla* (and when the Mmr is absent in *Pan*), the Fa appears more triangular (Fig. 4). In both *P. troglodytes* and *G. gorilla*, the Fa is not enclosed by an elevated Mmr, so it is "open" mesiolingually. At the distal margin of the tooth is the distal marginal ridge (Dmr), which, along with the Dpc and Tc, encloses the posterior fovea (Fp). The Fp of the P_3 occludes with the paracone of the P^3 in centric occlusion.

In contrast to the extant apes, human canines are reduced in size and are not honed. Given that all extant nonhuman catarrhines have a functional canine honing complex, we infer that the *Pan*-hominin last common ancestor must have also had a functional honing complex, which we therefore take to be the symplesiomorphic pattern for hominins. A reduction in canine size and the loss of honing are evident in the earliest hominins; for example, moderate canine reduction has been used to diagnose the earliest purported hominins from the late Miocene and early Pliocene (i.e., *Sahelanthropus tchadensis*, *Orrorin tugenensis*, *Ardipithecus kadabba*), though the morphology and function of the canine honing complex in some of these taxa are still poorly understood (Haile-Selassie, 2001; Senut et al., 2001; Brunet et al., 2002; Haile-Selassie et al., 2004, 2009; Semaw et al., 2005). No P_3s have been attributed to either *Sahelanthropus* or *Orrorin*; however, a P_3 attributed to *Ar. kadabba* (ASK-VP-3/403) has a "small" wear facet on its mesiobuccal face that resulted from occlusion with the maxillary canine, indicating that at least *some* of the earliest hominin individuals retained honing function, albeit in a reduced form (Haile-Selassie et al., 2004, 2009; Simpson et al., 2007). The situation is better known for *Ardipithecus ramidus*, in which all elements of the complex are known. The *A. ramidus* canines (especially the maxillary canine) are reduced in size,

Table 1
Abbreviations for morphological and directional terms.

Term	Abbreviation
Protoconid	Prd
Metaconid	Med
Mesial protoconid crest	Mpc
Distal protoconid crest	Dpc
Transverse crest	Tc
Mesial marginal ridge	Mmr
Distal marginal ridge	Dmr
Posterior fovea	Fp
Anterior fovea	Fa
Mesiodistal(ly)	MD
Buccolingual(ly)	BL

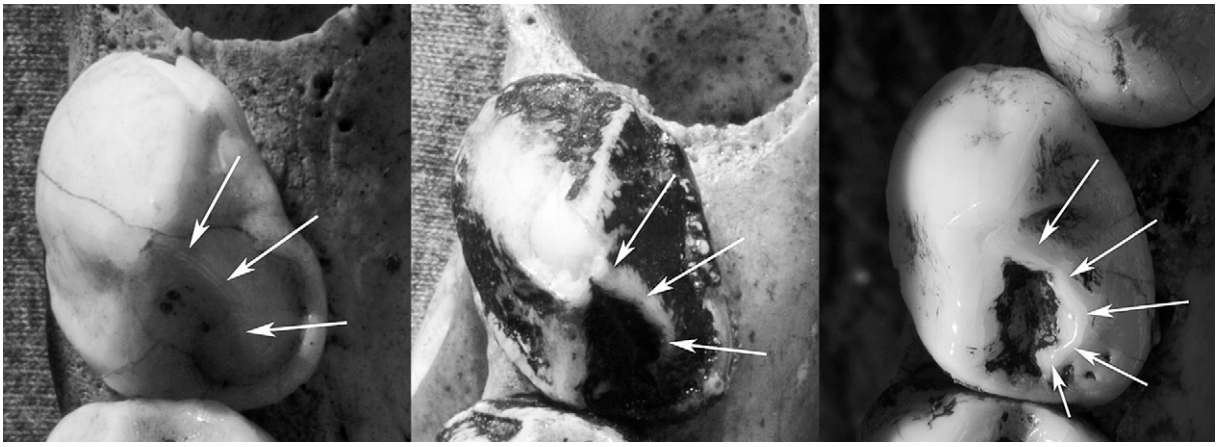

Figure 3. From left to right: Left P_3 *G. gorilla gorilla*, Left P_3 *G. gorilla gorilla*, Left P_3 *G. gorilla beringei*. The Tc of *G. gorilla* curves distally, as opposed to the condition in *P. troglodytes* in which the Tc is straight. The curved Tc is observed in both *G. gorilla gorilla* and *G. gorilla beringei*, indicating that it is not a population-level variant.

compared to those of extant apes, and there is no indication of honing wear on the canines or P_3 (Suwa et al., 2009). Though functionally derived, the P_3 of *Ar. ramidus* preserves much of the morphological feature set described above for *Pan* and *Gorilla*: the *Ar. ramidus* P_3 sample is uniformly unicuspid, the crests of the crown are sharp, the Tc is distolingually oriented, the Mmr remains unfused, and the mesiobuccal face projects inferiorly to an extent not seen in younger hominin species (White et al., 1994; see Fig. S14 in Suwa et al., 2009).

Compared to these earliest hominins, the genus *Australopithecus* is characterized by a further reduction in the absolute and relative size of the canines and a shift towards exclusively apical canine wear (Ryan and Johanson, 1989; Greenfield, 1990). *A. anamensis*, known from Kanapoi (4.2 Ma) and Allia Bay, Kenya (3.9 Ma), and Asa Issie, Ethiopia (4.1–4.2 Ma), is the oldest and most basal species so far allocated to the genus *Australopithecus* and is likely the phyletic ancestor of *A. afarensis* (Fig. 5) (Leakey et al., 1995; Ward et al., 2001; Kimbel et al., 2006; White et al., 2006). As in *Ar. ramidus*, the reduced *A. anamensis* canines do not participate in a honing complex but, as in *Ar. ramidus*, the *A. anamensis* P_3 is noted for its retention of plesiomorphic features. For example, *A. anamensis* P_3s uniformly lack a well-developed Med, any development of a lingual cusp is minimal and when present is a small "pyramid of enamel" (Kimbel et al., 2006) that is not different from the incipient Med that is occasionally observed in *P. troglodytes*. The *A. anamensis* P_3 Prd is tall and has sharp crests radiating from its tip; the Fa is open and only defined by a weakly developed Mmr (the components of which remain mostly unfused); and the major axis of the crown is obliquely set relative to the remainder of the postcanine teeth (Ward et al., 2001; Kimbel et al., 2006). In these respects, the P_3 of *A. anamensis* is plesiomorphic relative to younger congeneric species.

A. afarensis (3.0–3.8 Ma) temporally succeeds *A. anamensis*, its likely ancestor, and is best represented at the sites of Hadar, Ethiopia, and Laetoli, Tanzania (Fig. 5) (Kimbel and Delezene, 2009). The *A. afarensis* P_3 sample has long been noted for a marked absence of sectorial features and impressive morphological variation (e.g., crown size, root configuration, Tc prominence, Med presence/absence, etc.; see Fig. 6) (Kimbel and Delezene, 2009). Within the *A. afarensis* hypodigm, a mixture of plesiomorphic and apomorphic states are expressed for several characters; this "phylogenetic polymorphism" (Kimbel et al., 2004) provides evidence for the mosaic nature of the changes that occurred in the transformation of the hominin P_3 crown. Notable derived features include the occasional presence of a salient lingual cusp, the Med, which may be topographically separated from the Prd by a MD-oriented groove, the longitudinal groove (Fig. 6; White, 1977, 1980; Johanson et al.,

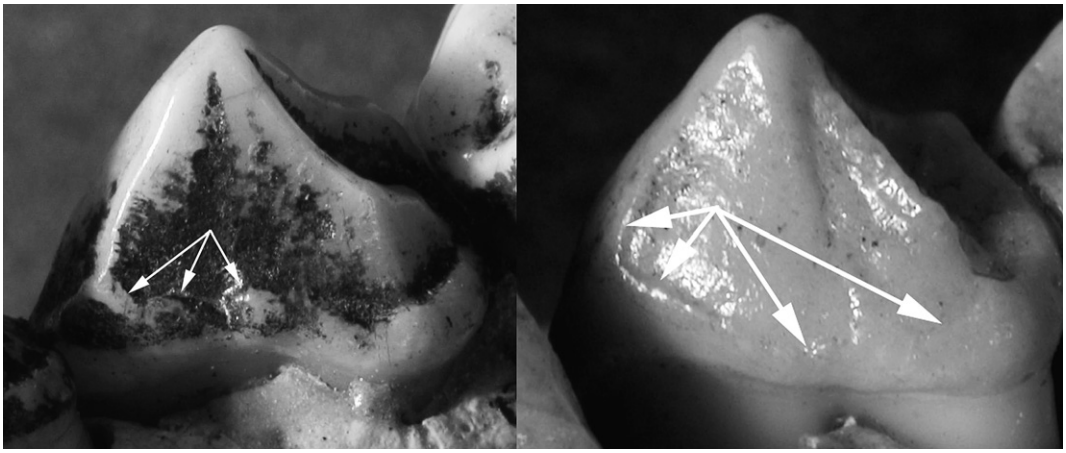

Figure 4. Lingual views of the Fa of a right P_3 of *G. gorilla* (on left) and *P. troglodytes* (on right). The white arrows indicate the Mmr; note the almost complete absence of the Mmr on the *G. gorilla* P_3 and the minimal development of the Mmr on the *P. troglodytes* P_3. The *G. gorilla* Fa appears as a triangle when viewed lingually, while the *P. troglodytes* Fa is more diamond-shaped due to the partial development of the Mmr.

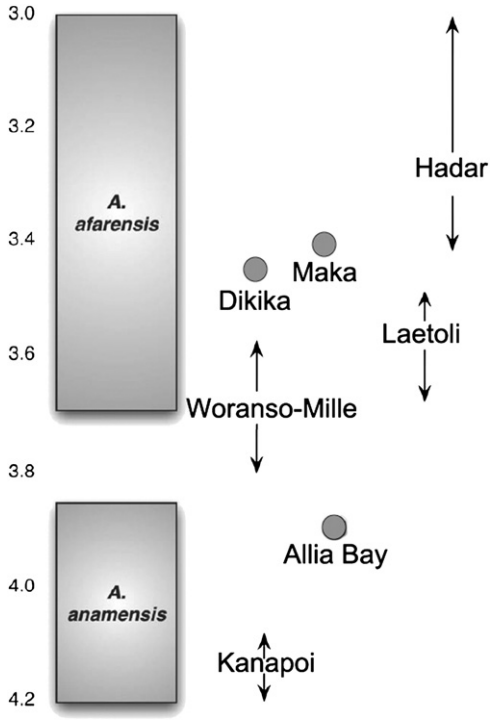

Figure 5. The geological ages of the *A. afarensis* and *A. anamensis* samples considered in this study; *y*-axis represents millions of years (modified after Kimbel et al. (2006)).

1982; Leonard and Hegmon, 1987), and, unlike in *Pan*, *Gorilla*, and *A. anamensis*, the crests of the *A. afarensis* P_3 crown (Tc, Mpc, Dpc, Mmr, and Dmr) are rounded rather than sharp (Johanson et al., 1982; Ward et al., 2001; Alemseged et al., 2005). Additional derived features characterize the *A. afarensis* Fa; in some *A. afarensis* specimens, the Mmr, Tc, and Mpc form an elevated rim that encloses the Fa, which is then manifested as a topographically low depression or "pit" when viewed occlusally (Johanson et al., 1982). The "pit-like" Fa of some *A. afarensis* specimens strongly contrasts with the open condition in *A. anamensis*, *P. troglodytes*, and *G. gorilla* (Fig. 6). The initial appearance of these derived features in the *A. afarensis* sample is particularly noteworthy because they uniformly characterize geologically younger hominin taxa.

The site of Woranso-Mille, Ethiopia (3.57–3.82 Ma), provides evidence for *Australopithecus* P_3 morphology during a poorly represented time period in hominin evolution. Three P_3s have been recovered from Woranso-Mille and one, ARI-VP-3/80 ($\geq$3.72 Ma), has published metrics (Deino et al., 2010; Haile-Selassie et al., 2010b). Haile-Selassie (2010) suggested that some specimens in the Woranso-Mille P_3 sample resemble *A. afarensis* (ARI-VP-2/95), while others show similarities to *A. anamensis* (ARI-VP-3/80 and MSD-VP-5/50), but are more derived in Fp expansion (MSD-VP-5/50) or Med development (ARI-VP-3/80) than the Kanapoi *A. anamensis* sample. Though the sample is morphologically intermediate, Haile-Selassie (2010) and Haile-Selassie et al. (2010b) suggested that sample's strongest phenetic similarity is to *A. anamensis* and that if *A. afarensis* and *A. anamensis* are considered distinct taxonomic entities, then the Woranso-Mille P_3s should be included in the *A. anamensis* hypodigm.

Though *A. afarensis* P_3 morphology has been discussed previously (e.g., Leonard and Hegmon, 1987; Suwa, 1990), continued collection of hominin fossils at Hadar (e.g., Kimbel et al., 2004; Kimbel and Delezene, 2009) and new discoveries at Dikika (Alemseged et al., 2005) and Maka (White et al., 1993, 2000), Ethiopia, have expanded the sample of P_3s attributed to this taxon. These finds have extended the temporal range of *A. afarensis* P_3s, including the youngest ($\sim$3.0 Ma; from the Kada Hadar-2 submember) and the oldest known ($\sim$3.42 Ma; from the Basal Member) P_3s from the Hadar Formation. Additionally, the sample previously available to Leonard and Hegmon (1987) and Suwa (1990) was skewed towards specimens from the A.L. 333 locality (5 of 12 Hadar P_3s at ca. 3.2 Ma) but fieldwork in Ethiopia has added 12 additional *A. afarensis* P_3s preserving occlusal morphology from localities other than A.L. 333.

The enlarged sample of early *Australopithecus* P_3s makes it possible to examine a wide range of issues at different biological scales, which we address here by analyzing quantitative variation in P_3 crown form across time and space in the earliest species of *Australopithecus*, *A. anamensis* and *A. afarensis*. To establish character polarity for P_3 crown features and to provide a comparative baseline for variation in biological samples, we compare early *Australopithecus* P_3 crown morphology to their extant African great ape outgroups, *Pan* and *Gorilla*. In the context of great ape comparative samples, we assess, in particular, the degree to which P_3 crown traits vary independently of one another spatiotemporally as a way of gaining insight into how the P_3 complex was transformed morphologically in these early hominins.

Materials

The extant great ape taxa *Gorilla gorilla gorilla* and *Pan troglodytes troglodytes* were each represented by sex-balanced samples of 15 males and 15 females from the Hamann-Todd Osteological Collection, Cleveland Museum of Natural History, and the collection of the Powell-Cotton Museum, Birchington, Kent, UK (Table 2). A sample size of 30 for each extant ape was chosen to approximately match that available for *A. afarensis*. Measurements of the fossil hominins were derived from original specimens housed at the National Museums of Kenya and the National Museum of Ethiopia, supplemented by high quality primary casts housed in the Institute of Human Origins, Arizona State University (Table 2).

All P_3s from Laetoli, Tanzania, and the sites of Hadar, Maka, and Dikika, Ethiopia, were considered in this analysis to be a part of the hypodigm of *A. afarensis*, ranging in age between 3.8 and 3.0 Ma. For *A. anamensis*, specimens from Kanapoi and Allia Bay, Kenya, were studied; these teeth range in time between 4.2 and 3.9 Ma. Because we have not examined the specimen firsthand, for analytical purposes we have chosen to not include ARI-VP-3/80 with either the *A. anamensis* (Kanapoi, Allia Bay) or *A. afarensis* (Hadar, Maka, Dikika, Laetoli) samples (Table 2), though we do include its published metrics in analyses that consider the lineage as a whole.

While *A. anamensis* and *A. afarensis* have been hypothesized to represent different parts of an anagenetic lineage (e.g., Kimbel et al., 2006; White et al., 2006), taxonomic diversity during this time period has been proposed. From the Koro Toro region of Chad, a small sample of *Australopithecus* ($n = 4$) is biochronologically dated to 3.0–3.5 Ma, a broad estimate that spans the entire age of the *A. afarensis*-bearing sediments of the Hadar Formation, Ethiopia (Brunet et al., 1996; Campisano and Feibel, 2008; Roman et al., 2008). The KT 12/H1 mandible was first referred to *A.* aff. *Australopithecus afarensis* (Brunet et al., 1995) and then subsequently designated the holotype of *Australopithecus bahrelghazali*, partially based on characters of P_3 root morphology (Brunet et al., 1996); however, many do not consider *A. bahrelghazali* to be diagnosably distinct from *A. afarensis* (e.g., White et al., 2000; Alemseged et al., 2005; Kimbel et al., 2006; but see Guy et al., 2008, who describe purportedly distinctive morphology in the symphyseal region of the *A. bahrelghazali* mandible). Taxonomic

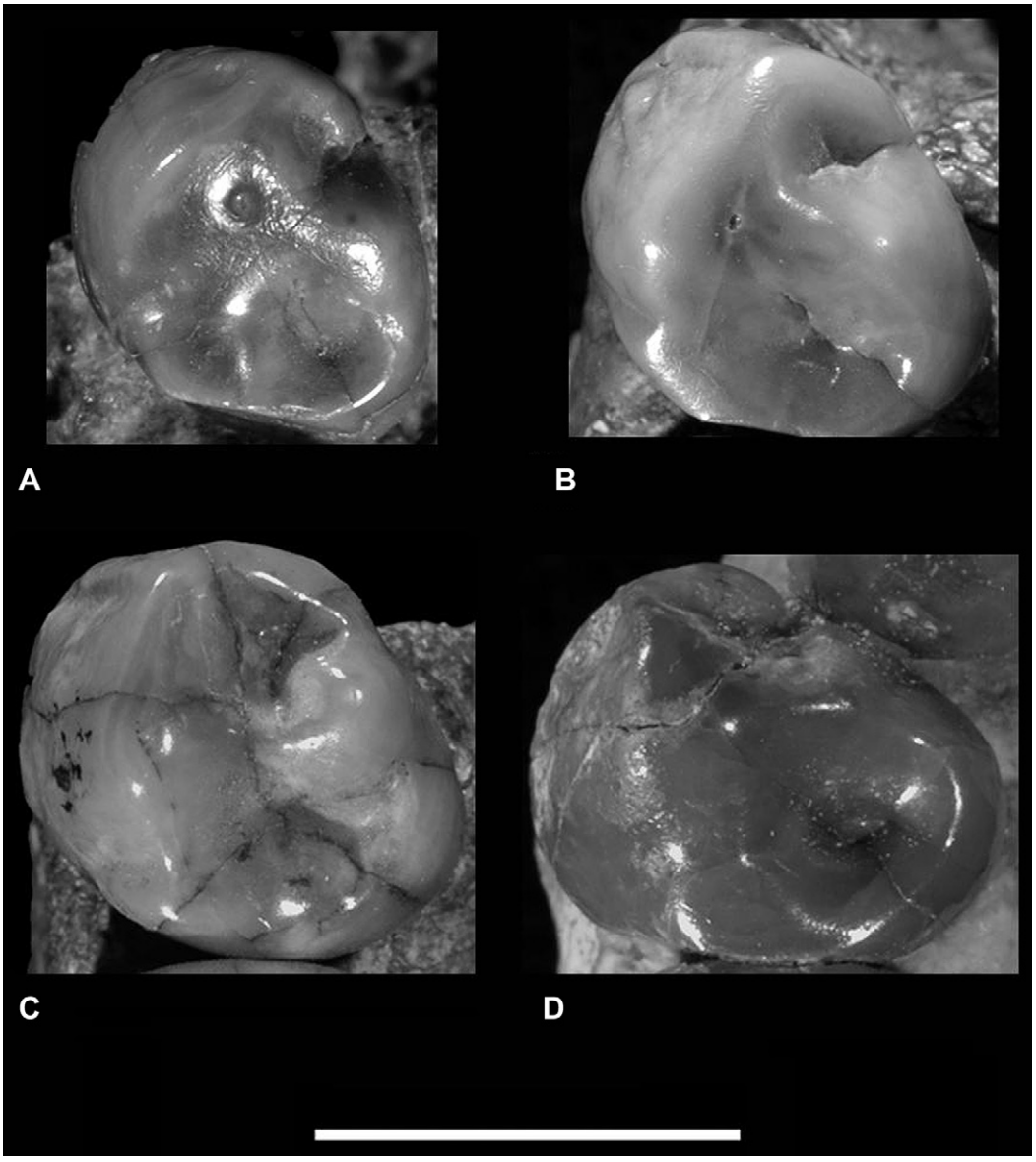

Figure 6. Variation in *A. afarensis* P_3 occlusal morphology as exemplified by A.L. 207-13 (A), A.L. 266-1 (B), A.L. 333w-1a (C), and A.L. 417-1 (D). Scale equals 1 cm. Note that these are not the photographs used to quantify occlusal morphology.

diversity has also been suggested by specimens from west of Lake Turkana, Kenya. From the Nachukui Formation, the Kataboi Member (>3.4 Ma) yielded the holotype (KNM-WT 40000) and the Lomekwi Member (<3.4 Ma) yielded the paratype (KNM-WT 38350) of *Kenyanthropus platyops* (Leakey et al., 2001). In addition to the *K. platyops* paratype, from the Lomekwi Member, several specimens (KNM-WT 8556, KNM-WT 16003, and KNM-WT 16006) dated to ~3.3 Ma have been attributed to *A. afarensis* or *A.* aff. *A. afarensis* (Brown et al., 2001). These Lomekwi Member specimens are similar in geological age to *A. afarensis* specimens from the Sidi Hakoma Member of the Hadar Formation. The mandibular fragment KNM-WT 8556, preserving most of the right postcanine dentition and the LP_3, is from the same collection area (LO-5) as the *K. platyops* paratype and is approximately the same geological age (see Fig. 4 in Leakey et al., 2001). Brown et al. (2001) highlighted apomorphic features of the KNM-WT 8556 P_3 shared with Hadar homologs, such as the presence of two well-defined cusps and general crown shape, but Leakey et al. (2001) pointed to specific morphological distinctions of KNM-WT 8556 relative to the *A. afarensis* hypodigm (though none of the distinctions relates to P_3 morphology). Leakey et al. (2001) did not attribute KNM-WT 8556 (or any of the other Lomekwi *A. afarensis*-like specimens) to *K. platyops*, but its taxonomic assignment is important because of its spatiotemporal association with the *K. platyops* material. In this study, we do not lump KT 12/H1 or KNM-WT 8556 with the *A. afarensis* sample; instead, we compare the P_3 crowns of KT 12/H1 and KNM-WT 8556 to the *A. afarensis* and *A. anamensis* hypodigms as a test of proposed hominin lineage diversity during the *A. afarensis* time range.

Methods

Metric features of the occlusal surface were acquired from scaled digital photographs (see Tables 3 and 4 and Figs. 7–9 for character descriptions) and were supplemented with caliper-based measures of MD length and BL breadth. The method of orienting each tooth to acquire a planimetric photograph followed Bailey and Lynch (2005), Bailey and Wood (2007), and Wood and Abbott (1983: 199), whereby the "plane of its cervical line, or base plane, is perpendicular to the

Table 2
Analyzed specimens. Hadar specimen A.L. 1496-1 was not included in any metric analysis, though we note some nonmetric features in this study. Specimens A.L. 1515-1 and ARI-VP-3/80 were not included in analyses of occlusal photographs, but were included in analyses of caliper-derived measurements.

P. troglodytes	*G. gorilla*	*A. afarensis*	*A. anamensis*	Other hominins
CAM 219 ♂	HTB 1077 ♂	A.L. 128-23[a,c]	KNM-ER 20432[a,c]	ARI-VP-3/80
M 52 ♂	HTB 1078 ♂	A.L. 198-1[a,c]	KNM-KP 29281[a,c]	KNM-WT 8556[b]
M 170 ♂	HTB 1196 ♂	A.L. 207-13[a,c]	KNM-KP 29284[a,c]	KT 12/H1[a]
M 278 ♂	HTB 1402 ♂	A.L. 266-1[a,c]	KNM-KP 29286[a,c]	
M 347 ♂	HTB 1403 ♂	A.L. 277-1[a,c]	KNM-KP 29287[a,c]	
M 401 ♂	HTB 1689 ♂	A.L. 288-1[a,c]	KNM-KP 30500[a,c]	
M 440 ♂	HTB 1709 ♂	A.L. 311-1[a,c]	KNM-KP 34725[a,c]	
M 707 ♂	HTB 1711 ♂	A.L. 315-22[b]		
M 719 ♂	HTB 1732 ♂	A.L. 333-10[a,c]		
M 988 ♂	HTB 1734 ♂	A.L. 333w-1a[a,c]		
Z IX 49 ♂	HTB 1751 ♂	A.L. 333w-46[a,c]		
Z VI 34 ♂	HTB 1780 ♂	A.L. 333w-58[a,c]		
Z VI 35 ♂	HTB 1847 ♂	A.L. 333w-60[b]		
Z VII 24 ♂	HTB 1860 ♂	A.L. 400-1[a,c]		
Z VII 25 ♂	HTB 1900 ♂	A.L. 417-1[a,c]		
M 105 3rd series ♀	HTB 1180 ♀	A.L. 437-2[b]		
M 148 3rd series ♀	HTB 1400 ♀	A.L. 438-2[a,c]		
M 169 2nd series ♀	HTB 1419 ♀	A.L. 440-1[a,c]		
M 181 ♀	HTB 1690 ♀	A.L. 655-1[a,c]		
M 382 ♀	HTB 1710 ♀	A.L. 822-1[a,c]		
M 449 ♀	HTB 1725 ♀	A.L. 1045-1[b]		
M 450 ♀	HTB 1740 ♀	A.L. 1496-1		
M 474 ♀	HTB 1764 ♀	A.L. 1515-1		
M 504 ♀	HTB 1782 ♀	DIK-2-1[b]		
M 506 3rd series ♀	HTB 1783 ♀	LH-2[a]		
M 655 ♀	HTB 1794 ♀	LH-3[a]		
M 664 ♀	HTB 1846 ♀	LH-4[a]		
M 676 ♀	HTB 1873 ♀	LH-14[a]		
M 886 ♀	HTB 1945 ♀	LH-24[a]		
M 986 ♀	HTB 1950 ♀	MAK-VP-1/12[a]		

[a] Fossil specimens for which occlusal photos were taken of a cast.
[b] Fossil specimen for which occlusal photos were taken of the original fossil.
[c] A specimen for which the original fossil was examined to ensure that the cast accurately reflects the recorded morphology.

optical axis of a camera." The software program ImageJ, which is freely available from the National Institutes of Health (http://rsb.info.nih.gov/ij/), was used to measure the area of polygons, projected distances between points, and angles between features. In Table 5, we report an assessment of the reliability of our measures using five *G. gorilla* and five *P. troglodytes* specimens. To test reliability, approximately five months after initially completing the study, LKD blindly rescaled and remeasured these 10 specimens.

Table 3
Points defined on the occlusal surface of the P_3 (also see Fig. 8).

Point	Definition
A	Prd tip
B	Point where a line from A along the Mpc intersects the mesial margin of the tooth
C	Point where a line from A along the Dpc intersects the distal margin of the tooth
D	Point where a line from A along the Tc intersects the lingual margin of the tooth

Table 4
Character descriptions (also see Fig. 8).

Character	Description
Projected Occlusal Area	The entire projected area of the profile of the crown as visible in occlusal view.
Relative Buccal Area	Ratio of area visible buccal to protoconid crests to the Projected Occlusal Area.
Relative Fa Area	Ratio of Fa Area to Projected Occlusal Area. The Fa Area is defined as the area visible lingual to the Mpc and mesial to the Tc.
Relative Fp Area	Ratio of Fp Area to Projected Occlusal Area. The Fp Area is defined as the area visible lingual to the Dpc and distal to the Tc.
Fa Area/Fp Area	Ratio of Fa Area to Fp Area.
MD Placement of Prd	Measured as the ratio of projected lengths of the Mpc (line BA) and the Dpc (line CA).
Angle BAD	Angle formed by Mpc (line AB) and Tc (line AD), open mesiolingually.
Angle CAD	Angle formed by the Dpc (line AC) and the Tc (line AD), open distolingually.
Relative Mesial Crown Breadth	Buccolingual breadth of mesial portion of crown, expressed as a percentage of the square root of Projected Occlusal Area. Mesial Crown Breadth is measured at ¼ of the length of the line BC, from the mesial crown perpendicular to line BC.
Relative Midcrown Breadth	Buccolingual breadth of midcrown, expressed as a percentage of the square root of Projected Occlusal Area. Midcrown Breadth is measured at ½ of the length of the line BC perpendicular to line BC.
Relative Distal Crown Breadth	Buccolingual breadth of distal crown, expressed as a percentage of the square root of occlusal area. The distal crown breadth is measured at ¾ of the length of the line BC perpendicular to line BC.
BC Length/Midcrown Breadth	Measured as the ratio BC Length/ Midcrown Breadth.
Mesial Crown Breadth/Distal Crown Breadth	Ratio of Mesial Crown Breadth to Distal Crown Breadth.
Mesial Crown Breadth/ Midcrown Breadth	Ratio of Mesial Crown Breadth to Midcrown Breadth.
Distal Crown Breadth/ Midcrown Breadth	Ratio of Distal Crown Breadth to Midcrown Breadth.

Intra-observer measurement error was in all cases less than 2% and in all but one case was less than 1.5% (see Table 5).

Differences among taxa were assessed using a permutation test (outlined in Manly, 2001), which uses a randomization procedure (sampling with no replacement). The permutation test was applied instead of a parametric test because it requires no assumption of normality and because it provides a more accurate assessment of statistical significance when small samples are considered. For normally distributed characters, the permutation test and *t*-test yield similar probabilities of statistical significance as sample sizes become larger (Todman and Dugard, 2001). In this study, each permutation test was constructed as a two-way test for mean difference and 1000 randomly constructed iterations were generated to form the distribution of mean differences to which the original mean difference was compared. The α-level for each pairwise comparison was set at 0.05; however, in instances where the *p*-value fell near the 0.05 cutoff (0.045–0.055), the *p*-value was recalculated using 5000 iterations (such instances are indicated). Given the large number of pairwise comparisons conducted for

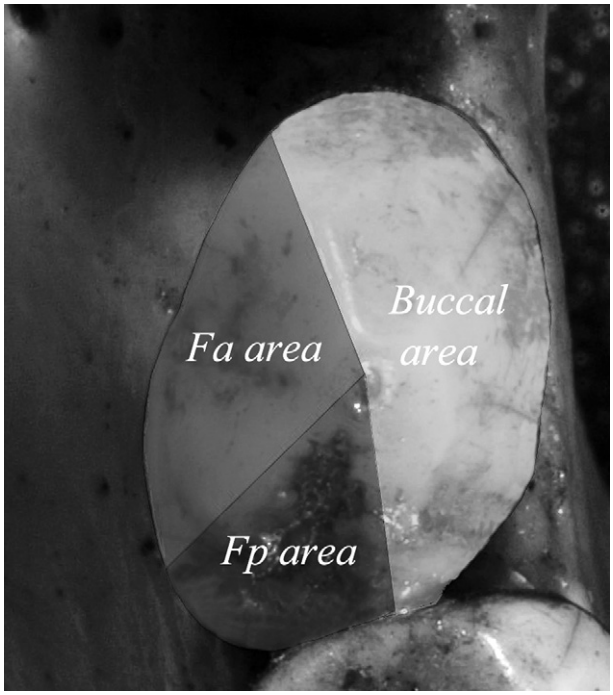

Figure 7. Right P_3 of *G. gorilla* illustrating the crown areas (Fa Area, Fp Area, Buccal Area) considered in this analysis. The three crown areas are defined by the location of the Mpc, Dpc, Prd, and the Tc.

each character (six, since four species were compared to one another), a Bonferroni correction was not used for hypothesis testing because it would generate an exceptionally stringent level for the rejection of the null hypothesis ($\alpha = 0.0083$ for six pairwise comparisons) and increase the probability of a Type II error (e.g., Moran, 2003; Garcia, 2004; Nakagawa, 2004). A rejection of the null hypothesis (no difference between sample means) was accepted when the *p*-value of the pairwise comparison was less than $\alpha = 0.05$.

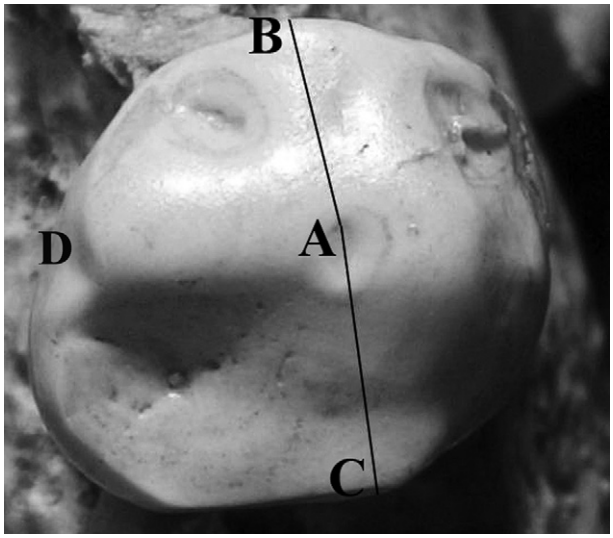

Figure 8. Right P_3 of *A. afarensis* illustrating the points used to define the projected lengths of the protoconid crests. Point A defines the tip of the Prd, point B defines the intersection of the mesial protoconid crest (Mpc) with the lingual crown margin, and point C defines the intersection of the distal protoconid crest (Dpc) with the distal crown margin.

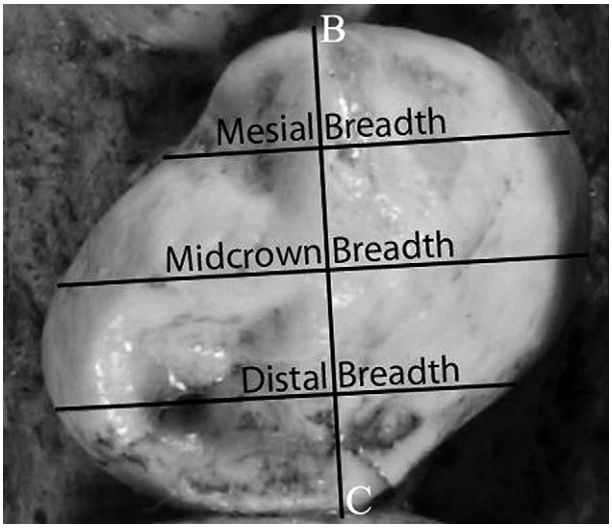

Figure 9. Crown widths and BC Length displayed on A.L. 128-23 (*A. afarensis*). The length of the line BC is divided by 4 and the crown's width is measured at ¼, ½, and ¾ of the length of the line BC. All crown widths are measured perpendicular to the line BC.

Although we do not consider the Bonferroni correction in hypothesis testing, we note in Tables 6 and 7 the comparisons that would be considered significant using the Bonferroni correction.

In addition to comparisons between species, subsamples of hominins were also compared to one another to investigate spatio-temporal differences between samples of *A. afarensis* and between *A. afarensis* samples and *A. anamensis*. Specimens of *A. afarensis* from Hadar, Dikika, and Maka, Ethiopia, were pooled and compared to the sample from Laetoli, Tanzania (see Fig. 5 for the relative ages of the sites). The *A. anamensis* sample was not divided into subsamples from Kanapoi and Allia Bay for statistical comparisons because only a single P_3 from Allia Bay is known; however, we highlight cases where the Allia Bay P_3 is distinct from that of the Kanapoi sample. The specimens tentatively assigned to *A. afarensis* (KNM-WT 8556 and KT 12/H1) were not pooled with the *A. afarensis* samples in any comparisons and were qualitatively compared to the distributions of the paradigmatic *A. afarensis* (Maka, Dikika, Hadar, Laetoli) and *A. anamensis* (Kanapoi, Allia Bay) samples.

Though statistical comparisons of variation, as expressed by the coefficient of variation (CV), are not the focus of our study, we do occasionally compare levels of variation. To do so, we utilized a bootstrapping procedure (sampling with replacement) to compare variation in the fossil assemblages to that present in extant samples.

Lockwood et al. (2000) investigated the evolution of the *A. afarensis* P_3 crown and identified potential trends in the reduction of MD length and occlusal area. Here, we revisit these trends in light of additions to the *A. afarensis* hypodigm (i.e., A.L. 437-2, A.L. 822-1, A.L. 1045-1, A.L. 1515-1, DIK-2-1, MAK-VP-1/12) that were not available to Lockwood et al. (2000) (although the mandible of A.L. 437-2 was included in the Lockwood et al. (2000) study, the A.L. 437-2 RP_3 was recovered in 2007) and also investigate the potential that temporal trends in P_3 crown evolution extend further into geological time to include the Woranso-Mille sample and the

Table 5
Repeatability study based on 5 *G. gorilla* and 5 *P. troglodytes* specimens.

Projected Occlusal Area	Fa Area	Fp Area	Buccal Area	Angle BAD	BC Length
0.50%	1.43%	1.55%	1.44%	1.05%	0.96%

Table 6
Ranges, means ($\bar{x}$), standard deviations (s), and sample sizes (n) for characters.

	P. troglodytes	*G. gorilla*	*A. afarensis*	Ethiopian *A. afarensis*	Laetoli *A. afarensis*	*A. anamensis*	KT 12/H1 (RP_3)	KNM-WT 8556 (LP_3)
Projected Occlusal Area (mm^2)	48.9–81.1 $\bar{x}$ = 64.4 s = 7.5 n = 30	104.5–192.8 $\bar{x}$ = 143.0 s = 25.0 n = 30	53.2–122.7 $\bar{x}$ = 77.9 s = 15.7 n = 26	53.2–122.7 $\bar{x}$ = 75.6 s = 15.4 n = 21	77.4–96.8 $\bar{x}$ = 90.9 s = 7.7 n = 5	71.8–79.7 $\bar{x}$ = 76.7 s = 3.5 n = 4	95.3	90.8
RelativeBuccal Area	0.37–0.51 $\bar{x}$ = 0.44 s = 0.04 n = 30	0.34–0.52 $\bar{x}$ = 0.43 s = 0.04 n = 30	0.25–0.50 $\bar{x}$ = 0.39 s = 0.07 n = 24	0.28–0.50 $\bar{x}$ = 0.39 s = 0.07 n = 19	0.25–0.44 $\bar{x}$ = 0.38 s = 0.08 n = 5	0.32–0.55 $\bar{x}$ = 0.45 s = 0.10 n = 4	0.33	0.30
Relative Fa Area	0.23–0.37 $\bar{x}$ = 0.29 s = 0.03 n = 30	0.18–0.34 $\bar{x}$ = 0.27 s = 0.04 n = 30	0.15–0.33 $\bar{x}$ = 0.21 s = 0.05 n = 24	0.15–0.30 $\bar{x}$ = 0.21 s = 0.04 n = 19	0.18–0.33 $\bar{x}$ = 0.24 s = 0.06 n = 5	0.20–0.29 $\bar{x}$ = 0.23 s = 0.04 n = 4	0.16	0.22
Relative Fp Area	0.21–0.36 $\bar{x}$ = 0.28 s = 0.04 n = 30	0.25–0.37 $\bar{x}$ = 0.30 s = 0.04 n = 30	0.33–0.55 $\bar{x}$ = 0.40 s = 0.05 n = 24	0.33–0.55 $\bar{x}$ = 0.40 s = 0.05 n = 19	0.35–0.41 $\bar{x}$ = 0.39 s = 0.03 n = 5	0.25–0.38 $\bar{x}$ = 0.32 s = 0.07 n = 4	0.50	0.48
Fa Area/Fp Area	0.67–1.55 $\bar{x}$ = 1.07 s = 0.23 n = 30	0.51–1.33 $\bar{x}$ = 0.90 s = 0.21 n = 30	0.32–0.86 $\bar{x}$ = 0.54 s = 0.12 n = 24	0.32–0.86 $\bar{x}$ = 0.52 s = 0.12 n = 19	0.44–0.80 $\bar{x}$ = 0.61 s = 0.13 n = 5	0.53–1.12 $\bar{x}$ = 0.79 s = 0.21 n = 5	0.32	0.45
Mesiodistal Placement of Prd	0.95–1.58 $\bar{x}$ = 1.19 s = 0.16 n = 30	0.72–1.42 $\bar{x}$ = 1.03 s = 0.19 n = 30	0.72–1.38 $\bar{x}$ = 0.93 s = 0.15 n = 24	0.72–1.38 $\bar{x}$ = 0.93 s = 0.15 n = 19	0.76–1.08 $\bar{x}$ = 0.94 s = 0.12 n = 5	0.93–0.98 $\bar{x}$ = 0.96 s = 0.02 n = 5	0.88	0.79
Angle BAD (degrees)	70–120 $\bar{x}$ = 101 s = 10 n = 30	81–117 $\bar{x}$ = 100 s = 10 n = 30	56–97 $\bar{x}$ = 78 s = 8 n = 25	56–97 $\bar{x}$ = 76 s = 8 n = 20	77–90 $\bar{x}$ = 83 s = 5 n = 5	85–111 $\bar{x}$ = 95 s = 10 n = 6	65	78
Angle CAD (degrees)	53–91 $\bar{x}$ = 72.5 s = 9.8 n = 30	53–89 $\bar{x}$ = 68.6 s = 8.6 n = 30	76–114 $\bar{x}$ = 92.0 s = 8.1 n = 24	81–114 $\bar{x}$ = 93.2 s = 8.0 n = 19	76–92 $\bar{x}$ = 87.5 s = 6.5 n = 5	70–87 $\bar{x}$ = 77.0 s = 6.5 n = 6	100	91
Relative Mesial Crown Breadth	0.79–1.01 $\bar{x}$ = 0.87 s = 0.06 n = 30	0.68–0.88 $\bar{x}$ = 0.80 s = 0.04 n = 30	0.81–1.07 $\bar{x}$ = 0.95 s = 0.06 n = 24	0.81–1.07 $\bar{x}$ = 0.95 s = 0.06 n = 19	0.87–0.99 $\bar{x}$ = 0.93 s = 0.05 n = 5	0.85–0.91 $\bar{x}$ = 0.88 s = 0.03 n = 4	0.91	0.91
Relative Midcrown Breadth	0.92–1.22 $\bar{x}$ = 1.07 s = 0.07 n = 30	0.96–1.16 $\bar{x}$ = 1.05 s = 0.05 n = 30	1.10–1.24 $\bar{x}$ = 1.16 s = 0.04 n = 24	1.10–1.24 $\bar{x}$ = 1.16 s = 0.04 n = 19	1.10–1.21 $\bar{x}$ = 1.17 s = 0.04 n = 5	1.12–1.19 $\bar{x}$ = 1.16 s = 0.03 n = 4	1.15	1.12
Relative Distal Crown Breadth	0.92–1.10 $\bar{x}$ = 1.01 s = 0.05 n = 30	0.92–1.08 $\bar{x}$ = 1.01 s = 0.05 n = 30	0.99–1.18 $\bar{x}$ = 1.07 s = 0.05 n = 24	0.99–1.18 $\bar{x}$ = 1.07 s = 0.05 n = 19	1.04–1.11 $\bar{x}$ = 1.08 s = 0.03 n = 5	1.06–1.11 $\bar{x}$ = 1.09 s = 0.02 n = 4	1.17	1.10
Relative BC Length	1.00–1.22 $\bar{x}$ = 1.12 s = 0.05 n = 30	1.08–1.24 $\bar{x}$ = 1.17 s = 0.04 n = 30	0.97–1.15 $\bar{x}$ = 1.06 s = 0.04 n = 24	0.97–1.11 $\bar{x}$ = 1.06 s = 0.04 n = 19	1.02–1.15 $\bar{x}$ = 1.06 s = 0.05 n = 5	1.07–1.08 $\bar{x}$ = 1.07 s = 0.01 n = 4	1.03	1.05
BC Length/Midcrown Breadth	0.83–1.33 $\bar{x}$ = 1.05 s = 0.11 n = 30	0.94–1.28 $\bar{x}$ = 1.12 s = 0.09 n = 30	0.78–1.04 $\bar{x}$ = 0.92 s = 0.06 n = 24	0.78–0.99 $\bar{x}$ = 0.92 s = 0.05 n = 19	0.84–1.04 $\bar{x}$ = 0.91 s = 0.08 n = 5	0.90–0.96 $\bar{x}$ = 0.93 s = 0.03 n = 4	0.90	0.94
MD Length/BL Breadth (caliper-based)	–	–	0.71–1.19 $\bar{x}$ = 0.90 s = 0.11 n = 29	0.71–1.14 $\bar{x}$ = 0.87 s = 0.09 n = 24	0.87–1.19 $\bar{x}$ = 1.00 s = 0.12 n = 5	0.82–0.96 $\bar{x}$ = 0.88 s = 0.07 n = 4	0.78	0.95
Mesial Crown Breadth/ Midcrown Breadth	0.73–0.90 $\bar{x}$ = 0.81 s = 0.05 n = 30	0.59–0.83 $\bar{x}$ = 0.76 s = 0.05 n = 30	0.72–0.89 $\bar{x}$ = 0.82 s = 0.05 n = 24	0.72–0.89 $\bar{x}$ = 0.82 s = 0.05 n = 19	0.76–0.82 $\bar{x}$ = 0.79 s = 0.02 n = 5	0.71–0.81 $\bar{x}$ = 0.76 s = 0.04 n = 4	0.79	0.81
Mesial Crown Breadth/ Distal Crown Breadth	0.74–1.02 $\bar{x}$ = 0.86 s = 0.06 n = 30	0.63–0.88 $\bar{x}$ = 0.79 s = 0.06 n = 30	0.74–0.98 $\bar{x}$ = 0.88 s = 0.06 n = 24	0.74–0.98 $\bar{x}$ = 0.89 s = 0.07 n = 19	0.83–0.89 $\bar{x}$ = 0.86 s = 0.03 n = 5	0.77–0.86 $\bar{x}$ = 0.81 s = 0.04 n = 4	0.78	0.83

Table 6 (*continued*)

	P. troglodytes	*G. gorilla*	*A. afarensis*	Ethiopian *A. afarensis*	Laetoli *A. afarensis*	*A. anamensis*	KT 12/H1 (RP_3)	KNM-WT 8556 (LP_3)
Distal Crown Breadth/ Midcrown Breadth	0.86–1.07 $\bar{x} = 0.95$ $s = 0.06$ $n = 30$	0.89–1.08 $\bar{x} = 0.96$ $s = 0.04$ $n = 30$	0.86–0.99 $\bar{x} = 0.92$ $s = 0.03$ $n = 24$	0.86–0.99 $\bar{x} = 0.92$ $s = 0.03$ $n = 19$	0.91–0.94 $\bar{x} = 0.92$ $s = 0.01$ $n = 5$	0.92–0.95 $\bar{x} = 0.94$ $s = 0.02$ $n = 4$	1.02	0.98

earlier *A. anamensis* samples from Kenya. Important for studies of temporal trends, DIK-2-1 (~3.42 Ma) and MAK-VP-1/12 (~3.4 Ma) are the geologically oldest P_3s known for Ethiopian *A. afarensis*, while A.L. 437-2 and A.L. 1515-1 (~3.0 Ma) are two recently recovered specimens from the youngest *A. afarensis*-bearing sediments at Hadar. At 3.72 Ma, ARI-VP-3/80 provides evidence for P_3 size and shape during a previously unsampled time period in the *A. anamensis*–*A. afarensis* lineage (Haile-Selassie, 2010; Haile-Selassie et al., 2010b). Following Lockwood et al. (2000), to investigate temporal trends we determined the statistical significance of the Γ statistic using a bootstrapping procedure (see Lockwood et al. (2000) for a more detailed description of the methodology). Given the large sample size available for the combined sample of *A. anamensis* and *A. afarensis*, we used 5000 randomizations and report the two-tailed probabilities of significance.

In order to visualize groupings among specimens and to explore the similarity among species and specimens to one another, a principal components analysis (PCA) was performed (Johnson and Wichern, 2007). The 15 log-transformed characters describing occlusal morphology used to create the PCA include measures of different scale (angles and ratios) with different variances; therefore, the principal components were calculated from the correlation matrix of the 15 variables using Statistica v7.1 (StatSoft, Inc., 2005); no characters expressing raw "size" were included in the PCA.

Results

Projected Occlusal Area

This variable measures the entire visible area of the P_3 crown in occlusal view (Table 4 and Fig. 7); that is, the projected area circumscribed by the visible profile of the crown. For this variable, the mean areas decrease in the series *G. gorilla* > *A. afarensis* > *A. anamensis* > *P. troglodytes* (Table 6) and all pairwise comparisons are significant except for the comparison of the two hominin taxa to one another (Table 7). Of interest is the large difference between the mean of the female and male *G. gorilla* samples (male mean = 161.7 mm^2; female mean = 124.4 mm^2; $p < 0.001$), which is reflected by an Index of Sexual Dimorphism (ISD = male mean/female mean) of 1.30. Dimorphism is present, but is much less pronounced, in *P. troglodytes* (male mean = 66.8 mm^2; female mean = 62.0 mm^2; $p = 0.080$; ISD = 1.08).

Compared to other taxa in this study, size variation in *A. afarensis* is remarkable. The DIK-2-1 P (122.7 mm^2) is the largest *A. afarensis* P_3 and is much larger than the second largest, LH-3 (96.8 mm^2), while A.L. 128-23 (53.5 mm^2) and A.L. 315-22 (53.2 mm^2) occupy the low end of the *A. afarensis* size range. In contrast to *A. afarensis*, the smaller *A. anamensis* sample has a much narrower range (Table 6). The large range of *A. afarensis* P_3 size is reflected in the max/min ratio: for *A. afarensis* it is 2.3, for *G. gorilla* it is 1.8, for *P. troglodytes* it is 1.7, and for *A. anamensis* it is 1.1. Extensive P_3 size variation also yields a large CV for *A. afarensis* (20.1), which is significantly greater than that of *P. troglodytes* (CV = 11.7; $p < 0.001$) and nearly significantly greater than the more dimorphic *G. gorilla* (CV = 17.5; $p = 0.055$). The *A. anamensis* CV (4.6) is much smaller. Among the *A. afarensis* samples, the Ethiopian CV (20.9) is much greater than the Laetoli CV (8.5). The *A. afarensis* CV (the Ethiopian sample in particular) is greatly affected by the very large DIK-2-1 crown; when the CV is recalculated without DIK-2-1 it drops to 17.1 for the entire sample and 16.2 for the Ethiopian sample.

While the CVs reported here for Projected Occlusal Area seem high relative to general standards of variation based on MD and BL linear measures, CVs for areas are about twice that observed for linear measures. To illustrate this, the CVs for the square root of Projected Occlusal Area are predictably lowered to the following: *A. afarensis* (10.0), Ethiopian *A. afarensis* (10.2), Laetoli *A. afarensis* (4.4), *G. gorilla* (8.8), *P. troglodytes* (5.9), and *A. anamensis* (2.3), which are similar to caliper-derived linear measures (e.g., Kimbel and Delezene, 2009; see also Suwa, 1990). Therefore, our reported CVs for Projected Occlusal Area reflect biological reality, are consistent with those observed for caliper-derived linear measures of the crown, and are not an artifact of the methodology used to capture the Projected Occlusal Area.

Table 7
p-values for pairwise comparisons of species; those *p*-values <0.05 are bolded and italicized. '*' indicates a comparison in which the *p*-value fell in the range 0.045–0.055 when 1000 iterations are used to calculate the *p*-value; in such cases, the reported *p*-value is based on a randomization utilizing 5000 iterations. '†' indicates a comparison that would be significant using a Bonnferonni adjustment (i.e., $p < 0.0083$).

	G. gorilla/*P. troglodytes*	*G. gorilla*/*A. afarensis*	*G. gorilla*/*A. anamensis*	*P. troglodytes*/*A. anamensis*	*P. troglodytes*/*A. afarensis*	*A. afarensis*/*A. anamensis*
Projected Occlusal Area	***<0.001***†	***<0.001***†	***<0.001***†	***0.001***†	***<0.001***†	0.858
Relative Buccal Area	0.700	***0.005***†	0.402	0.460	***0.002***†	0.104
Relative Fa Area	***0.024***	***<0.001***†	0.070	***0.002***†	***<0.001***†	0.622
Relative Fp Area	***0.008***†	***<0.001***†	0.397	***0.048****	***<0.001***†	***0.009***
Fa Area/Fp Area	***0.003***†	***<0.001***†	0.336	***0.016***	***<0.001***†	***0.003***†
MD Placement of Prd	***0.002***†	***0.039***	0.353	***0.005***†	***<0.001***†	0.738
Angle BAD	0.584	***<0.001***†	0.350	0.170	***<0.001***†	***0.001***†
Angle CAD	0.115	***<0.001***†	***0.026***	0.313	***<0.001***†	***<0.001***†
Relative Mesial Breadth	***<0.001***†	***<0.001***†	***0.003***†	0.753	***<0.001***†	***0.018***
Relative Midcrown Breadth	0.361	***<0.001***†	***<0.001***†	***0.019***	***<0.001***†	0.869
Relative Distal Breadth	0.844	***<0.001***†	***0.004***†	***0.001***†	***<0.001***†	0.651
Relative BC Length	***<0.001***†	***<0.001***†	***<0.001***†	0.109	***<0.001***†	0.545
BC Length/Midcrown Breadth	***0.015***	***<0.001***†	***<0.001***†	***0.035***	***<0.001***†	0.688
Mesial Breadth/Midcrown Breadth	***<0.001***†	***<0.001***†	0.963	***0.026***	0.863	***0.038***
Mesial Breadth/Distal Breadth	***<0.001***†	***<0.001***†	0.503	0.181	0.129	***0.031***
Distal Breadth/Midcrown Breadth	0.501	***0.001***†	0.252	0.630	***0.035***	0.400

Previous analyses indicated that Laetoli P_3s are larger than those from Hadar (e.g., White, 1977, 1980; Suwa, 1990; Lockwood et al., 2000). This difference is observed in this study as well, as the mean for the Laetoli sample is larger than that of the Ethiopian (Hadar, Dikika, Maka) sample (Table 6); however, the difference between the two samples does not quite reach the level of statistical significance (Table 8). When the Laetoli sample is compared to only the 1970s sample of Hadar P_3s (mean = 72.9 mm^2) the difference is significant (p-value = 0.009). Currently, the Ethiopian *A. afarensis* P_3 size range encompasses the entire range of the Laetoli sample (Table 6); the recently discovered A.L. 437-2 P_3 (93.8 mm^2) is among the largest Ethiopian *A. afarensis* P_3s and DIK-2-1 (122.7 mm^2) is the largest known. Though the Laetoli mean is larger than that of the Ethiopian *A. afarensis* sample, this results from an overrepresentation of large teeth in the numerically small Laetoli P_3 sample, as has been noted by others (e.g., White, 1985; Suwa, 1990).

Both KT 12/H1 and KNM-WT 8556 fall in the upper end of the distribution of P_3 size for *A. afarensis* and above that observed in *A. anamensis* (Table 6). The KT 12/H1 P_3 is 1.12 standard deviations above the *A. afarensis* mean, exceeded in size by only DIK-2-1 and LH-3. The KNM-WT 8556 P_3 is only 0.82 standard deviations larger than the *A. afarensis* mean.

Relative crown areas

We analyzed three areas in terms of relative size: Relative Buccal Area, Relative Fa Area, and Relative Fp Area (Table 4 and Fig. 7). Each projected area was divided by Projected Occlusal Area to express the relative area occupied by the feature of interest.

For Relative Buccal Area the means are arranged as *A. anamensis* > *P. troglodytes* > *G. gorilla* > *A. afarensis* (Table 6). *A. afarensis* has a significantly smaller Relative Buccal Area than the extant taxa (Table 7); the extant apes, with the mesiobuccal extension forming the canine honing surface, have a larger portion of the crown devoted to the area buccal to the protoconid crests. As has been noted by others (e.g., Alemseged et al., 2005; Haile-Selassie, 2010), the *A. anamensis* Prd is situated in the center of the tooth in the BL dimension, exposing a large area buccal to the Prd crests. This large Relative Buccal Area is a reflection of the strongly-unicuspid nature of the *A. anamensis* P_3s; among the *A. afarensis* sample, unicuspid teeth (e.g., A.L. 128-23, A.L. 288-1) also have large Relative Buccal Areas. Both KT 12/H1 and KNM-WT 8556 are within the *A. afarensis* range and at the lower limit of or below that seen in *A. anamensis*.

For Relative Fa Area (Table 4 and Fig. 7), the means are arranged as *P. troglodytes* > *G. gorilla* > *A. anamensis* > *A. afarensis* (Table 6). *A. afarensis* has a significantly smaller Relative Fa Area than both ape taxa while *A. anamensis* has a significantly smaller Relative Fa Area than *P. troglodytes*, but not *G. gorilla* (Table 7). When viewed occlusally, the two hominin taxa have relatively small Fas and cannot be distinguished using this metric. Though no statistically significant differences are observed among the *A. afarensis* samples (Table 8), relatively large Fas are observed in the Laetoli sample (see also Haile-Selassie, 2010). The Relative Fa Area of the KT 12/H1 P_3 falls within the *A. afarensis* range and below that seen in *A. anamensis*, while the Relative Fa Area of KNM-WT 8556 is within both the *A. afarensis* and *A. anamensis* ranges.

For Relative Fp Area (Table 4 and Fig. 7), the means are arranged as *A. afarensis* > *A. anamensis* > *G. gorilla* > *P. troglodytes*, indicating that *A. afarensis* has the largest Relative Fp Area (Table 6). All interspecific pairwise comparisons are significant except for that of *A. anamensis* to *G. gorilla* (Table 7). Among the hominin samples, the Ethiopian *A. afarensis* sample has a significantly larger Relative Fp Area than *A. anamensis*, while the Laetoli Relative Fp Area falls just short of significance when compared to *A. anamensis*; that is, the difference between *A. afarensis* and *A. anamensis* when the Laetoli and Ethiopian samples are pooled is largely driven by the difference between the Ethiopian and *A. anamensis* samples (Table 8). The *A. bahrelghazali* P_3 and the Lomekwi P_3 fall within the *A. afarensis* range, above that seen in *A. anamensis*, indicating an *A. afarensis*-like expanded posterior crown relative to *A. anamensis*.

The ratio Fa Area/Fp Area describes the size of the Fa relative to the Fp (Table 4 and Fig. 7). Values larger than one indicate that the Fa occupies a larger projected area than the Fp. For this variable, the means are ordered as *P. troglodytes* > *G. gorilla* > *A. anamensis* > *A. afarensis*, indicating that *A. afarensis* has the smallest Fa Area, relative to Fp Area, of any taxon analyzed (Table 6). All pairwise comparisons are significantly different except for the comparison of *A. anamensis* to *G. gorilla* (Table 7). In the extant apes, the Fa Area is large relative to both Projected Occlusal Area and Fp Area. Although the Fa of *A. anamensis* is small in projected area, like that of *A. afarensis*, the Fp does not dominate the lingual portion of the crown as it does in *A. afarensis* (Kimbel et al., 2006). As discussed above, the lingually-placed Prd of *A. anamensis* expands the portion of the crown visible buccally and reduces the absolute size of both lingual foveae; however, the plesiomorphic dominance of Fa Area over Fp Area is preserved in *A. anamensis*. This variable also reveals a distinction between the Kanapoi sample of *A. anamensis* and the single P_3 from Allia Bay (KNM-ER 20432). The mean of the Kanapoi sample ($n = 4$) is 0.86 and the range is 0.76–1.12, while the value observed for KNM-ER 20432 is 0.53, a value that falls near the *A. afarensis* mean (Table 6; see also Kimbel et al., 2006). Among the hominins, the Ethiopian sample of *A. afarensis* is significantly different from the *A. anamensis* sample while the Laetoli sample is not; the *A. anamensis* and Laetoli samples express a more plesiomorphic ratio of Fa Area to Fp Area than the Ethiopian sample of *A. afarensis* (Table 8). The KT 12/H1 ratio falls at the lower limit of the *A. afarensis* range and well below that of *A. anamensis*; its Fa Area is among the smallest relative to Fp Area. The KNM-WT 8556 ratio falls within the *A. afarensis* distribution and below that seen in *A. anamensis* (Table 6).

Table 8
p-values for pairwise comparisons of hominin samples; p-values <0.05 are bolded and italicized. '†' indicates a comparison would be significant using a Bonnferonni adjustment (i.e., $p < 0.017$).

	Ethiopia–Laetoli	Ethiopia – *A. anamensis*	Laetoli – *A. anamensis*
Projected Occlusal Area (mm^2)	0.057	0.872	***0.033***
Relative Buccal Area	0.677	0.125	0.228
Relative Fa Area	0.203	0.419	0.746
Relative Fp Area	0.595	***0.012***†	0.063
Fa Area/Fp Area	0.165	***0.001***†	0.135
Mesiodistal Placement of Prd	0.919	0.747	0.761
Angle BAD (degrees)	0.097	<***0.001***†	***0.038***
Angle CAD (degrees)	0.147	***0.001***	***0.022***
Relative Mesial Crown Breadth	0.365	***0.025***	0.189
Relative Midcrown Breadth	0.774	0.933	0.720
Relative Distal Crown Breadth	0.893	0.670	0.613
Relative BC Length	0.897	0.537	0.794
BC Length/Midcrown Breadth	0.959	0.686	0.786
MD length/BL Breadth (caliper-based)	***0.012***	0.920	0.118
Mesial Crown Breadth/Midcrown Breadth	0.262	***0.028***	0.168
Mesial Crown Breadth/Distal Crown Breadth	0.320	***0.037***	0.077
Distal Crown Breadth/Midcrown Breadth	0.957	0.460	0.220

Protoconid position

The variable Relative MD Placement of the Prd was examined by calculating the ratio of the projected lengths of the protoconid crests (Mpc and Dpc) (the ratio of the lengths of the lines AB and AC; Fig. 8, Tables 3 and 4). Since the Mpc and Dpc meet at the Prd and tend to run along the MD axis of the crown, this variable measures the relative MD position of the Prd. Index values greater than 1.0 indicate that the Mpc has a longer projected length than the Dpc.

Reflecting an elongated mesial face devoted to the honing facet, both extant apes have mean values for Relative MD Placement of the Prd that are greater than 1.0, while that of *A. anamensis* is slightly less than 1.0 and *A. afarensis* has the smallest mean (Table 6); the Prd is most mesially situated in *A. afarensis*. *A. anamensis* mean is not significantly different from those of *G. gorilla* or *A. afarensis*, while all other pairwise comparisons are significantly different (Table 7). Both KT 12/H1 and KNM-WT 8556 have a mesially-situated Prd and fall within the *A. afarensis* distribution and at the lower limit of or below that of *A. anamensis* (Table 6).

As the crests that define the occlusal foveae originate from the Prd, the placement of the Prd is an important determinant of the size of the regions that are used in this analysis. When all specimens are pooled, the correlations between the Relative MD Placement of the Prd and Relative Fa Area ($r = 0.60$, $p < 0.001$) and Relative Fp Area ($r = -0.56$, $p < 0.001$) are significant. As expected, as the Prd becomes more mesially positioned in *Australopithecus* the relative size of the Fa is restricted and the Fp is correspondingly expanded.

Orientation of the transverse crest

As discussed above, two components of the plesiomorphic feature set observed in *Pan* and *Gorilla* are a relatively large Fa and a relatively small Fp. The MD placement of the Prd plays an important role in determining the size of these foveae. Additionally, *Pan* and *Gorilla* differ from most hominins in the distolingual orientation of the Tc. To determine the extent to which hominin samples diverge from this plesiomorphic state, we quantify the orientation of the Tc relative to the Mpc and the Dpc and report correlations between relative foveae area and the orientation of the Tc.

The angle between the Tc and Mpc is measured as the Angle BAD (Tables 3 and 4 and Fig. 8) and the taxon means decrease in the series *P. troglodytes* > *G. gorilla* > *A. anamensis* > *A. afarensis* (Table 6). *A. afarensis* is significantly different from all other taxa (Table 7); that is, the Tc is most acutely angled in *A. afarensis*. Both KT 12H/1 and KNM-WT 8556 share an acutely oriented Tc with *A. afarensis* (Table 6).

The Angle CAD (Tables 3 and 4 and Fig. 8) measures the orientation of the Tc relative to the Dpc. For this angle, the taxon means are arranged *A. afarensis* > *A. anamensis* > *P. troglodytes* > *G. gorilla*, indicating that the Tc is the most acutely angled, relative to the Dpc, in *G. gorilla* (Table 6). All pairwise comparisons involving *A. afarensis* are significant, as is the comparison of *A. anamensis* to *G. gorilla* (Table 7). Again, KT 12/H1 and KNM-WT 8556 fall outside the *A. anamensis* range and within the *A. afarensis* distribution.

As the Tc defines the border between the two occlusal foveae, the orientation of the Tc affects the relative size of the foveae. To illustrate this relationship, when all specimens are pooled, the correlations between the Angle BAD and Relative Fa Area ($r = 0.56$, $p < 0.001$) and Relative Fp Area ($r = -0.65$, $p < 0.001$) are significant. In *Pan*, *Gorilla*, and *A. anamensis*, the Tc courses distolingually, forming an obtuse angle with the Mpc and an acute angle with the Dpc, creating a large Fa Area relative to Fp Area, while *A. afarensis*, KT 12/H1, and KNM-WT 8556 have more mesially rotated Tcs (and correspondingly small Fa Area relative to Fp Area), occupying the other end of the morphological spectrum.

Relative buccolingual breadth and mesiodistal length

We have demonstrated that relative to the plesiomorphic condition, the length of the MPC in *A. afarensis* is reduced in proportion to the DPC and that the Fa is reduced in area compared to the Fp. Ward et al. (1999, 2001) (see also Kimbel et al., 2006) noted that the *A. anamensis* P_3 crown sample is elongated MD relative to geologically younger hominin taxa and that the Hadar sample of *A. afarensis* is reduced in MD length relative to the Laetoli sample of *A. afarensis* (for *A. afarensis*, see also Lockwood et al., 2000). We used several metrics to determine the significance of differences in relative MD length and BL Breadth in our samples. From occlusal photographs, crown breadths were measured perpendicular to the line BC at ¼, ½, and ¾ of the length of line BC (Fig. 9). The crown breadths were divided by the square root of Projected Occlusal Area to express relative widths of the crown. Similarly, the ratio of BC Length to the square root of Projected Occlusal Area was considered, as was the ratio BC Length/Midcrown Breadth. For *A. afarensis* and *A. anamensis* only, caliper-derived measures of MD length and BL breadth were used to consider the ratio MD/BL. Caliper-derived measures were included for the hominins because they were obtained differently than length and breadth from occlusal photographs; measures derived from occlusal photographs utilize landmarks of the crown to define lengths and widths. The inclusion of the caliper-derived measures makes it possible to compare results to previous analyses of *A. afarensis* and *A. anamensis* P_3 crown morphology (e.g., Lockwood et al., 2000; Kimbel et al., 2006).

The measures of relative crown breadth derived from occlusal photographs (Relative Mesial Crown Breadth, Relative Midcrown Breadth, Relative Distal Crown Breadth, Relative BC Length, and BC Length/Midcrown Breadth) indicate that the *G. gorilla* crown is the most elongated MD (relative to BL Breadth) and that the *A. afarensis* crown is the most broad BL (relative to MD length). *G. gorilla* is significantly different from *P. troglodytes* for three measures (Relative Mesial Crown Breadth, Relative BC Length, and BC Length/Midcrown Breadth). For all measures, *A. afarensis* is significantly different from both *P. troglodytes* and *G. gorilla* (Table 7). Similarly, *A. anamensis* is significantly different from both *G. gorilla* (all measures of relative breadth and length) and *P. troglodytes* (all variables except for Relative BC Length and Relative Mesial Crown Breadth). Using these measures, the hominin taxa are only significantly different from one another in Relative Mesial Crown Breadth (as discussed below, *A. afarensis* P_3s often have a well-developed Mmr that fills out the mesiolingual portion of the crown, making this portion of the crown broader than in *A. anamensis*). This difference is largely driven by the comparison of the Ethiopian sample to *A. anamensis*, as the Laetoli sample is not significantly different from *A. anamensis* (Table 8). The isolated specimens KT 12/H1 and KNM-WT 8556 fall within the range of values observed for *A. anamensis* and *A. afarensis*, indicating similarly MD-reduced crowns. The Relative Distal Crown Breadth of KT 12/H1 is within the *A. afarensis* distribution, but is among the largest values observed in the analysis. The KT 12/H1 crown is relatively broad distally, which partially explains the relatively large Fp Area identified earlier.

Using caliper-derived measures, a significant difference is observed between the Laetoli and Ethiopian *A. afarensis* samples for the ratio MD/BL (Table 8). As noted previously (White, 1985; Suwa, 1990; Lockwood et al., 2000), the Laetoli P_3 sample is more MD elongated, relative to BL Breadth, than the Ethiopian specimens (Fig. 10); however, neither *A. afarensis* sample differs significantly from *A. anamensis* (Table 8). As noted by Haile-Selassie (2010) and Haile-Selassie et al. (2010b), the Woranso-Mille P_3 ARI-VP-3/80 has the highest crown shape index (1.26) for any published *A. afarensis* or *A. anamensis* P_3 crown. The crown shape index for the KNM-WT

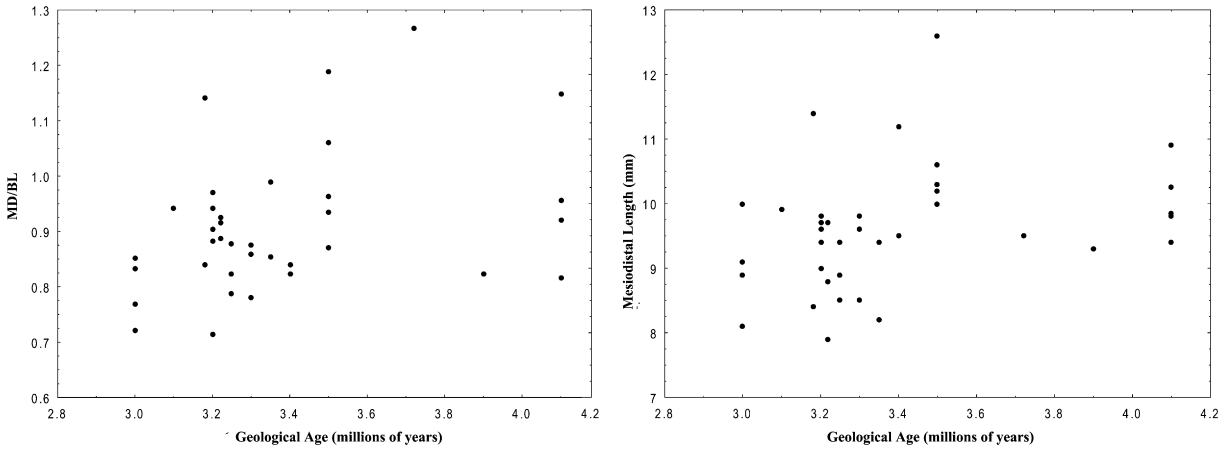

Figure 10. Temporal trends for crown shape index (MD/BL) and MD length for *A. anamensis* and *A. afarensis*.

8556 P_3 falls within the ranges of both *A. afarensis* and *A. anamensis*, while that of KT 12/H1 falls towards the low end of the *A. afarensis* range and outside that of *A. anamensis* (Table 6). Implications for temporal trends in crown shape are discussed further below.

The comparisons of relative MD length and BL Breadth demonstrate that *G. gorilla* and the hominins occupy opposite extremes of the morphological spectrum. *G. gorilla* has a crown that is on average longer MD than it is wide BL, while the hominins have on average a relatively broad crown. Specimens of *A. afarensis* from Hadar, Maka, and Dikika, and the *A. afarensis*-affiliated specimens, KT 12/H1 and KNM-WT 8556, are the BL broadest relative to MD length.

Crown shape

The means for the ratio of Mesial Crown Breadth to Midcrown Breadth are ordered as *A. afarensis* > *P. troglodytes* > *G. gorilla* = *A. anamensis* (Table 6). All pairwise comparisons are significant except for the comparisons of *A. anamensis* to *G. gorilla* and *P. troglodytes* to *A. afarensis* (Table 7). As discussed for Relative Mesial Crown Breadth, in the *A. afarensis* crowns the development and prominence of the Mmr creates a more filled-out mesiolingual corner than in *A. anamensis*, which lacks a prominent Mmr. The difference between the hominin taxa is largely driven by the comparison of the Ethiopian *A. afarensis* sample to *A. anamensis*, which is significant, as the comparison between the Laetoli sample and *A. anamensis* is not (Table 8). Reflecting the well-developed Mmr present in both specimens, both KT 12/H1 and KNM-WT 8556 are within the *A. afarensis* distribution and near the upper limit of the *A. anamensis* range (Table 6).

For the ratio of Mesial Crown Breadth to Distal Crown Breadth, the means are arranged as *A. afarensis* > *P. troglodytes* > *A. anamensis* > *G. gorilla* (Table 6). The comparisons of *G. gorilla* to *P. troglodytes*, *G. gorilla* to *A. afarensis*, and *A. afarensis* to *A. anamensis* are significant (Table 7). Again, this variable captures the differences in the mesiolingual crown profile described above. The Ethiopian *A. afarensis* sample is significantly different from *A. anamensis*, but the Laetoli sample is not (Table 8). Reflecting its broad distal crown, the KT 12/H1 P_3 is within, but near the lower limit of, the *A. afarensis* distribution. The ratio for KNM-WT 8556 is below the *A. afarensis* mean, but is within both the *A. afarensis* and *A. anamensis* distributions (Table 6).

For the ratio of Distal Crown Breadth to Midcrown Breadth, the means are arranged as *G. gorilla* > *P. troglodytes* > *A. anamensis* > *A. afarensis* (Table 6). For this variable, only the comparisons of *A. afarensis* to *G. gorilla* and *P. troglodytes* are significantly different (Table 7). The KT 12/H1 P_3 is above both the *A. afarensis* and *A. anamensis* distributions, while the KNM-WT 8556 P_3 is within, but near the upper limit of, the *A. afarensis* distribution and above the *A. anamensis* distribution. Both KNM-WT 8556 and KT 12/H1 have relatively broad distal crowns, with KT 12/H1 being more exaggerated (Table 6).

Temporal trends in P_3 crown evolution

As part of a larger study of metric variation and evolution in *A. afarensis*, Lockwood et al. (2000) investigated temporal trends in *A. afarensis* P_3 crown morphology and identified temporally vectored reductions in MD length and occlusal area. Here, we report tests for temporal change in P_3 MD length, BL breadth, crown shape index (MD/BL), and crown size (MD*BL). We used the metric MD*BL (measured with calipers) to assess crown size trends since recently recovered specimens that are important for interpreting temporal trends (i.e., A.L. 1515-1 and ARI-VP-3/80) were not included in analyses of planimetric photographs. Results are reported separately for the *A. afarensis* hypodigm and for the combined samples of the *A. anamensis* and *A. afarensis* lineage (Table 9).

The results for *A. afarensis* strengthen the conclusions of Lockwood et al. (2000). Significant temporal change is observed in MD length and crown shape (MD/BL) to become BL broader, relative to MD length, in the Ethiopian *A. afarensis* sample (Table 9 and Fig. 10). The results of this study do differ from those of Lockwood et al. (2000) in some respects: whereas we found a significant trend towards decreased MD/BL, they did not; also, we found no significant reduction in crown size, whereas Lockwood et al. (2000) did. As Lockwood et al. (2000) found a significant trend for MD reduction, but not BL reduction, over time, they inferred that crown shape must have also changed over time despite finding no significant change in the MD/BL ratio. The temporal trend for shape change now reaches statistical significance because two more MD short but BL broad specimens from Hadar (A.L. 437-2, A.L. 1515-1) have been added to the youngest temporal interval (KH-2 submember). The significance of this trend can be seen by contrasting the shape of the Laetoli and KH-2 P_3s; though both samples tend to be similar in overall crown size, there is no overlap in MD length between the two samples (Fig. 10). The trend towards crown size reduction is not significant in the current study because some of the youngest P_3s added to the hypodigm are large. Although, as discussed previously, DIK-2-1 (152.3 mm^2) is the largest *A. afarensis* P_3, the two new KH-2 submember P_3s (A.L. 437-2, A.L. 1515-1) have crown sizes (114.7 mm^2 and 130 mm^2, respectively) that make them among the

Table 9
Temporal change in *A. anamensis*–*A. afarensis* P_3 crown size and shape. Those correlations that are significant ($p < 0.05$) are bolded and italicized.

	n	Rank correlation	2-Tailed product probability
A. afarensis			
P_3 MD	30	$r_s = -0.357$	***0.018***
P_3 BL	30	$r_s = -0.092$	0.415
P_3 MD/BL	30	$r_s = -0.278$	***<0.001***
P_3 MD*BL	30	$r_s = -0.229$	0.347
A. anamensis–A. afarensis			
P_3 MD	37	$r_s = -0.376$	***0.014***
P_3 BL	36	$r_s = -0.032$	0.726
P_3 MD/BL	36	$r_s = -0.296$	***0.003***
P_3 MD*BL	36	$r_s = -0.211$	0.097

largest known *A. afarensis* P_3s. In the Lockwood et al. (2000) study, the Laetoli P_3s were both the oldest and the largest; in the current study, the inclusion of large P_3s from the youngest portion of the Hadar Formation reduces the leverage that Laetoli P_3 size has on the appearance of a temporal trend in crown size reduction. Though crown size remains taphonomically biased in the numerically small Laetoli sample (White, 1985; Suwa, 1990; Lockwood et al., 2000), it is difficult to envision a taphonomic distortion in crown shape (Lockwood et al., 2000); the geologically oldest *A. afarensis* P_3s differ in shape from the youngest, regardless of their size.

Including the earlier *A. anamensis* samples (Kanapoi, Allia Bay) and the Woranso-Mille P_3 (ARI-VP-3/80) does not reveal strong evidence that temporal trends in P_3 morphology extended over the known duration of the *A. anamensis*–*A. afarensis* lineage. When the analysis was restricted to only *A. afarensis* (Hadar, Maka, Dikika, Laetoli), significant reduction in MD length and shape change result in a MD-shorter crown (relative to BL Breadth). While it is true that the *A. anamensis* P_3 is longer MD than the Hadar *A. afarensis* sample, there is no evidence for a change in MD length or crown shape (MD/BL) between *A. anamensis* and the geologically oldest *A. afarensis* P_3s (Table 8, Fig. 10). However, the elongated crown of the Woranso-Mille P_3 (attributed to *A. anamensis* by Haile-Selassie (2010) and Haile-Selassie et al. [2010b]) shows that MD-elongated crowns (relative to BL Breadth) are not restricted to Laetoli *A. afarensis* and suggests that the significance of the observed trends when *A. anamensis* and *A. afarensis* are combined into a single analysis largely reflects the strength of the changes that occurred subsequent to 3.6 Ma.

Principal components analysis

A principal components analysis (PCA) was conducted on 90 individuals (30 *P. troglodytes*, 30 *G. gorilla*, 24 *A. afarensis*, 4 *A. anamensis*, KNM-WT 8556, and KT 12/H1) using the correlation matrix of 15 log-transformed variables, derived from occlusal photographs, which describe the shape of the P_3 (see Table 10 for factor loadings); no characters capturing raw size were included in the PCA. Two principal components contain variables with factor loadings greater than |0.7| and these two principal components explain 64.6% of the variance in the sample (Table 10).

When displayed graphically, the combination of PC1 and PC2 separates specimens into previously recognized species (Fig. 11). For PC1, high positive loadings characterize Fa Area/Fp Area, Angle BAD, Relative BC Length, and BC Length/Midcrown Breadth; high negative loadings relate to Relative Fa Area, Angle CAD, Relative Mesial Crown Breadth, Relative Midcrown Breadth, and Relative Distal Crown Breadth. Those individuals with broad crowns BL (relative to MD length), small Relative Fa Area, small Fa Area relative to Fp Area, and a mesially-rotated Tc have negative scores on

Table 10
Factor loadings for the first three principal components from the PCA based on 90 individuals (all variables are log transformed). Bolded loadings are >|0.700|.

Relative Buccal Area	0.417	0.123	0.081
Relative Fa Area	**0.702**	0.219	0.411
Relative Fp Area	**−0.814**	−0.239	−0.385
Fa Area/Fp Area	**0.842**	0.254	0.442
Angle BAD	**0.842**	−0.032	0.184
Angle CAD	**−0.824**	−0.071	−0.029
Mesiodistal Placement of Prd	0.412	0.243	0.495
Relative Mesial Crown Breadth	**−0.803**	0.545	0.083
Relative Midcrown Breadth	**−0.822**	−0.126	0.487
Relative Distal Crown Breadth	−0.653	−0.528	0.312
Relative BC Length	**0.856**	−0.070	−0.378
BC Length/Midcrown Breadth	**0.878**	0.039	−0.458
Mesial Crown Breadth/ Midcrown Breadth	−0.237	**0.800**	−0.351
Mesial Crown Breadth/Distal Crown Breadth	−0.421	**0.895**	−0.110
Distal Crown Breadth/ Midcrown Breadth	0.396	−0.413	−0.316
Proportion of total variance explained	*48.24*	*16.39*	*11.52*
Cumulative percentage of variance explained		*64.64*	*76.15*

PC1. The extensive overlap between *G. gorilla* and *P. troglodytes* and the fact that *G. gorilla* and the largest hominin P_3s (KT 12/H1, DIK-2-1, A.L. 437-2, LH-3) lie at opposite ends of PC1 indicate that PC1 is not a "size" component. For PC2, high positive loadings occur for Mesial Crown Breadth/Midcrown Breadth and Mesial Crown Breadth/Distal Crown Breadth.

Reflecting the results of the univariate analysis and capturing the distinction between the plesiomorphic feature set of the extant great apes and the derived condition of the geologically youngest hominins, on PC1 *P. troglodytes* and *G. gorilla* overlap extensively while *A. afarensis*, KNM-WT 8556, and KT 12/H1 occupy the opposite end of the morphometric spectrum. PC 1 is best interpreted as a component reflecting a continuum from plesiomorphic to apomorphic as those specimens with MD-elongated crowns, relatively large Fas, relatively small Fps, and distolingually-oriented

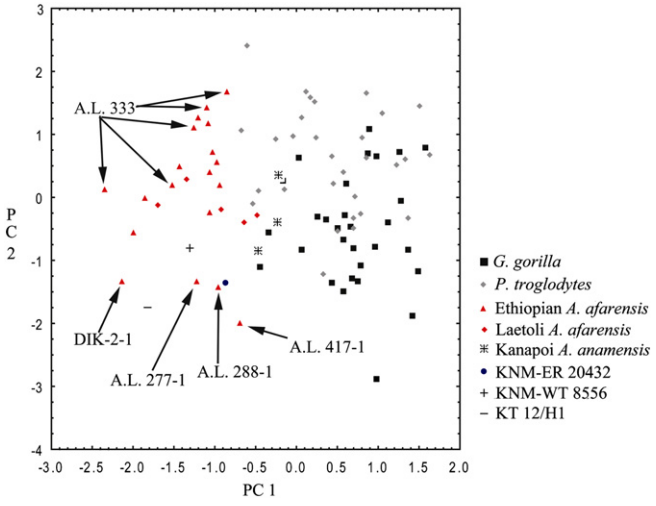

Figure 11. Plot of factor scores for PC1 and PC2 based on 15 log-transformed variables derived from occlusal photographs. PC1 shows that the extant taxa and Ethiopian *A. afarensis* lie at opposite ends of a morphocline. *Australopithecus anamensis* and Laetoli *A. afarensis* lie between Ethiopian *A. afarensis* and the extant taxa on PC1. PC2 does little to separate taxa more than PC1 does by itself. Note that A.L. 277-1, A.L. 288-1, and A.L. 417-1 are unicuspid *A. afarensis* specimens that plot near KNM-ER 20432.

Tcs plot to the right of PC 1 and those with the opposite configuration (reduced Fa, expanded Fp, mesially-rotated Tc, relatively broader crown BL) plot to left. On PC1, three of five Laetoli specimens (LH-3, LH-14, LH-24) are scattered among the Ethiopian *A. afarensis* specimens, while two of five (LH-2, LH-4) are at the fringe of the extant ape distribution. This result is not unexpected, as the Laetoli specimens tend to be more MD elongated and, among the *A. afarensis* specimens, they feature the largest Relative Fa Area (see Table 6). Additionally, reflecting their more plesiomorphic configuration (small Relative Fp Area, large Fa Area/Fp Area ratio, distolingually-oriented Tc) relative to *A. afarensis*, on PC1 the Kanapoi *A. anamensis* specimens overlap the negative end of the *P. troglodytes* and *G. gorilla* distributions. The Allia Bay P_3, KNM-ER 20432, is within the *A. afarensis* distribution (in a region of phenotype space shared with unicuspid Hadar specimens) due to its *A. afarensis*-like ratio of Fa Area/Fp Area and relative BL width. Metric and nonmetric features that differ between this specimen and the Kanapoi sample of *A. anamensis* P_3s are addressed in more detail in Discussion (see also Kimbel et al., 2006). As PC2 does little to separate groups more than PC1 does alone, it mostly captures intraspecific and not interspecific variation.

The PCA makes it possible to assess the morphological cohesiveness of the *A. afarensis* P_3 sample. It reveals that the A.L. 333 specimens ($n = 5$) are quite similar to other *A. afarensis* specimens on PC1, but have high scores on PC2, reflecting the fact that all of them have a well-developed Mmr that creates a "filled-out" mesiolingual crown contour (see also Leonard and Hegmon, 1987; Suwa, 1990: 99–100). Thus, the mesial crowns of the A.L. 333 specimens are relatively broad compared to their midcrown and distal crown dimensions. The A.L. 333 individuals are not unique in this regard within the *A. afarensis* hypodigm, as other *A. afarensis* specimens plot with the A.L. 333 sample (Fig. 11).

The PCA also permits an assessment of the similarity of the KNM-WT 8556 and KT 12/H1 P_3s to other early *Australopithecus* P_3s. Specimen KNM-WT 8556 plots within the *A. afarensis* cluster, while KT 12/H1 plots nearest *A. afarensis* specimen DIK-2-1. The position of these hominin P_3s with the *A. afarensis* sample reflects the results of the univariate analysis, which indicated few instances in which KNM-WT 8556 differs from paradigmatic examples of *A. afarensis*. The KT 12/H1 P_3 was shown to have a broad distal crown (relative to mesial and midcrown measurements), which explains its low score on PC2.

Discussion

Morphology of the extant African apes

Despite a large difference in P_3 crown size, *P. troglodytes* and *G. gorilla* share a suite of features that are well established as plesiomorphic for the hominin P_3. These include presence of a tall, MD-centered Prd; lack of a well-developed Med; minimal to no development of the Mmr, yielding a mesiolingually "open" Fa; Fa that is often larger in projected area than the Fp; rootward mesiobuccal enamel extension that forms the honing surface for the maxillary canine; and a Tc that is distolingually oriented. Despite these shared similarities, the two African apes are distinguishable both metrically and nonmetrically. They differ in variables reflecting relative crown length and width (relatively broader crown in *P. troglodytes*), the MD placement of the Prd (more distal in *P. troglodytes*) and crown shape (Table 7). Though not discussed here in a statistical framework, consistent nonmetric differences are also observed. *G. gorilla* specimens express a Tc that curves distally, instead of running straight distolingually as is always observed in our *P. troglodytes* sample (Figs. 1–3). The curved Tc observed in our *G. gorilla gorilla* sample is also observed in *G. gorilla beringei*, indicating that it is not a subspecific, or population-level, variant observed only within our western lowland gorilla sample (Fig. 3). Similarly, the curved Tc is not observed in *P. troglodytes verus* or *Pan troglodytes schweinfurthii*. The Mmr of *G. gorilla* is often absent, while it is often present but poorly developed in *P. troglodytes* (Fig. 4; see also Suwa, 1990). These metric and nonmetric differences demonstrate that a single invariant morphotype does not characterize the extant African ape P_3.

Some of the features shared by *P. troglodytes* and *G. gorilla* represent functional attributes related to canine honing (e.g., tall Prd, mesiobuccal enamel extension); however, some shared features are not obviously functionally linked to canine honing (Relative Fp Area, Tc orientation) and these characters vary among *Pan*, *Gorilla*, and other hominoid taxa that also possess a honing complex. For example, relative to the African apes, *Pongo pygmaeus* and *Pongo abelii* have a more transversely-oriented Tc and a correspondingly expanded Fp (unpublished observations of the authors). The *Pongo* Prd is tall and centrally placed along the MD axis of the tooth (as in *Pan* and *Gorilla*), leaving an absolutely large Fa in place, but the Fp is absolutely larger than in African apes (Fig. 12). Among the extant apes, interspecific differences in P_3 occlusal form are mainly in features unrelated to honing (e.g., Mmr development, Fp size, Tc orientation) while the core features of the canine honing complex are preserved among taxa. Dietary differences observed between the hominines (e.g., Stanford and Nkurunungi, 2003; Remis, 2006; Taylor, 2006; Yamagiwa and Basabose, 2006) may be implicated in the morphological differences observed in the distal part of the crown.

In the metric and nonmetric features that distinguish *G. gorilla* and *P. troglodytes*, *P. troglodytes* is more similar to hominins and, therefore, represents a better morphotype from which to derive

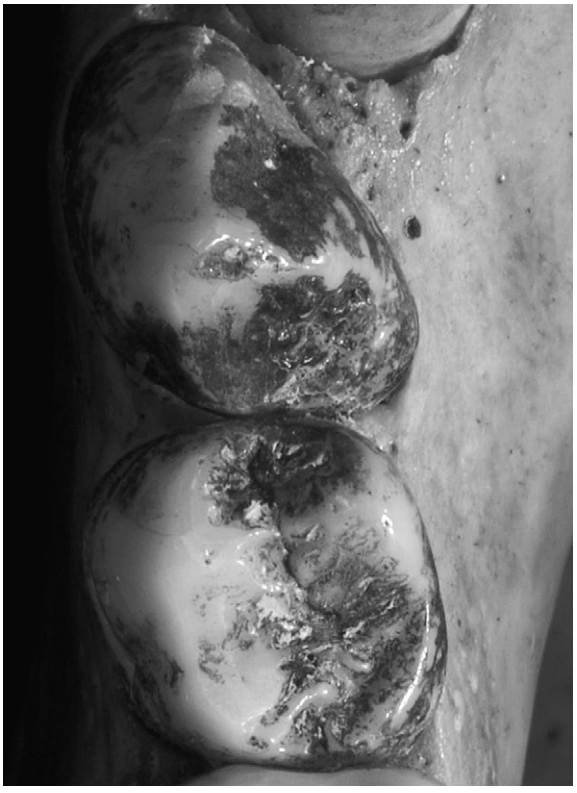

Figure 12. Left P_3 and P_4 of *Po. pygmaeus*. Compared to the African apes, the P_3 and P_4 of *Pongo* are characterized by absolutely larger Fps. For the P_3, this results from a more transversely positioned Tc in *Pongo*.

early hominin P_3 crown morphology. The possibility that *G. gorilla* differs from the hominins and *P. troglodytes* as a result of dietary differences is discussed above; regardless of their functional importance, if the features of the *G. gorilla* crown represent the plesiomorphic states for the tooth, then the features shared by *P. troglodytes* and the hominins would be synapomorphies. The distally-curved Tc observed in *G. gorilla* is not observed in any other extant or extinct hominoid taxon that we are familiar with (i.e., *Proconsul*, *Kenyapithecus*, *Dryopithecus*, *Sivapithecus*, *Ouranopithecus*, *Pongo*, *Hylobates*) suggesting that the character state is autapomorphic for *Gorilla*. The Mmr is minimally developed in *Hylobates*, *Proconsul* (e.g., KNM-RU 2036A, KNM-RU 2087), *Kenyapithecus* (e.g., KNM-FT 45), *Dryopithecus* (e.g., IPS 23), and *Sivapithecus* (e.g., GSP 15000). The Mmr of *Pongo* is slightly better developed than in other hominoid taxa, but its general absence among hominoids suggests that Mmr absence is likely the plesiomorphic state for *Pan* and *Gorilla* (see also Suwa, 1990). So, given the minimal development of the Mmr occasionally observed in *Pan*, then *some* development of the Mmr may prove to be a synapomorphy of the *Pan* + hominin clade. It is of interest that Haile-Selassie et al. (2004, 2009) noted the presence of the buccal segment of the Mmr on a 5.6–5.8 million-year-old P_3 of *Ar. kadabba* (ASK-VP-3/403).

The P_3 crown of A. anamensis

A. anamensis is the oldest (4.2–3.9 Ma) and phylogenetically most basal species of *Australopithecus* so far known (Leakey et al., 1995, 1998; Ward et al., 2001). Although the loss of canine honing is already evident in 4.4 million-year-old *Ar. ramidus* (White et al., 1994; Suwa et al., 2009), the P_3 of *A. anamensis* retains a number of plesiomorphic features shared with extant African apes. For example, *A. anamensis* P_3s are uniformly unicuspid; the Prd is tall and has sharp crests radiating from its tip; the Fa is open (i.e., only defined by a weakly-developed Mmr) and often larger than the Fp in projected area; the major axis of the P_3 crown is obliquely set relative to the remainder of the postcanine dentition; and the Tc is more distolingually oriented than is seen in geologically younger *Australopithecus* taxa (Ward et al., 2001; Kimbel et al., 2006). Significant departures from *Pan* and *Gorilla* include a smaller Relative Fa Area, a larger Relative Fp Area, and a MD-shorter and BL-broader crown, all derived features shared with subsequent hominin taxa. While not considered here in a statistical framework, nonmetric departures of the *A. anamensis* P_3 from *Pan* and *Gorilla* conditions include a more prominent Mmr (compare Figs. 4 and 13), though it is notably weaker and less elevated than in any later hominin species. The nonmetric and metric features that differentiate *A. anamensis* from the extant apes also characterize *A. afarensis*, in which they are further elaborated.

Spatiotemporal differences are observed within the *A. anamensis* hypodigm. The Kanapoi P_3 sample is demonstrably more plesiomorphic than the single known Allia Bay P_3 (KNM-ER 20432) (Kimbel et al., 2006). For example, KNM-ER 20432 differs from the Kanapoi sample in its crown shape, which is more BL expanded relative to MD length (Fig. 10), and the ratio Fa Area/Fp Area, which indicates the KNM-ER 20432 Fa is small relative to Fp size. Additionally, when viewed lingually, both Kanapoi *A. anamensis* and some *P. troglodytes* P_3s have a Fa that is defined by a centrally-placed Prd, a weakly-developed Mmr, whose components trend inferiorly from their origins towards the cervix of the tooth, and a sharp, highly-sloped Tc. Though the Mmr of the Kanapoi specimens is more prominent than in *Pan*, the similar slopes of the Mmr and Tc result in a Fa that is diamond-shaped when viewed lingually (Figs. 4 and 13). The Fa of KNM-ER 20432, in contrast, does not possess the pronounced diamond-shaped Fa because the buccal segment of the Mmr is more prominent, elevated, and does not trend inferiorly as in Kanapoi specimens (Kimbel et al., 2006). For KNM-ER 20432, this configuration yields a triangular Fa when viewed lingually. Though KNM-ER 20432 is worn, the contrast with KNM-KP 29281, a worn P_3 from Kanapoi, is clear (Fig. 13). The elevation of the buccal segment of the Mmr in the Allia Bay P_3 is a synapomorphy shared with *A. afarensis.* Given the departures of KNM-ER 20432 from the Kanapoi sample, it is clear why KNM-ER 20432 clusters with *A. afarensis* in the PCA (Fig. 11; see also Kimbel et al., 2006).

The P_3 crown of A. afarensis

The *A. afarensis* P_3 sample has long been noted to vary in size and the expression of derived features (e.g., root number and configuration; Med presence/absence; development of the longitudinal groove; development of the lingual segment of the Mmr; prominence and fusion of the Mmr; crown shape; crown obliquity) (White 1977, 1980; Johanson et al., 1982; Leonard and Hegmon, 1987; Suwa, 1990). However, this variation does not obscure the sharp differences between the P_3s of *A. afarensis* and *A. anamensis* (Tables 6–8, Fig. 11). Given the various combinations of plesiomorphic and apomorphic traits observed in the *A. afarensis* P_3 sample, it is tempting to dichotomize the hypodigm into derived and primitive morphs (e.g., Coppens, 1977; Olson, 1985; Leonard and Hegmon, 1987). If these morphs represented real biologically differentiated samples, then variation in occlusal form within the *A. afarensis* hypodigm could represent multiple species (e.g., Olson, 1985) or sexual dimorphism (e.g., Leonard and Hegmon, 1987); however, arguments based on the 1970s sample of *A. afarensis* pointed out that variation in shape and the presence/absence of nonmetric features cuts across purported taxonomic and sex-related boundaries (Kimbel et al., 1985) and, as well, is unrelated to differences in P_3 size. New discoveries, discussed below, expand the variation observed in the *A. afarensis* hypodigm while solidifying the morphological cohesiveness of the sample (White et al., 2000; Kimbel et al., 2006; Kimbel and Delezene, 2009). An appreciation of variation reveals that there is no cohesive, derived "package" of morphological features; the mosaic expression of derived and primitive character states in the *A. afarensis* hypodigm reveals the independent nature of many of the changes that occurred during the transformation of the hominin P_3 crown (see further discussion below).

A few examples illustrate the mosaicism present in the *A. afarensis* sample. Variation in the presence/absence of a Med is independent of variation in the size of the Fa. It might be expected that those specimens with discrete Meds would also have small Fas, but specimens in the Laetoli sample show that this is not necessarily true. For example, LH-2, LH-3, and LH-14 all have well-developed Meds but retain large Fas compared to the Ethiopian *A. afarensis* sample (see also Haile-Selassie, 2010). In these Laetoli specimens, the prominence of the Mmr is not necessarily an effect of having a discrete Med, as they also have Meds but less prominent Mmrs than are usually seen in the Ethiopian sample.

The independent expression of derived character states of the P_3 can also be addressed by examining the pattern of character-state changes in the *A. anamensis–A. afarensis* lineage. The constellation of derived features that characterizes the Ethiopian *A. afarensis* sample are: small Relative Fa Area, large Relative Fp Area, prominent Mmr, occasional fusion of the Mmr, mesial shift in Prd, frequent presence of a salient Med, relatively short crown MD, and mesially-rotated Tc. If the hominin sample that represents the *A. anamensis–A. afarensis* lineage is divided into four time-successive samples (Kanapoi, Allia Bay, Laetoli, Ethiopia), it is apparent that the character states that constitute the derived

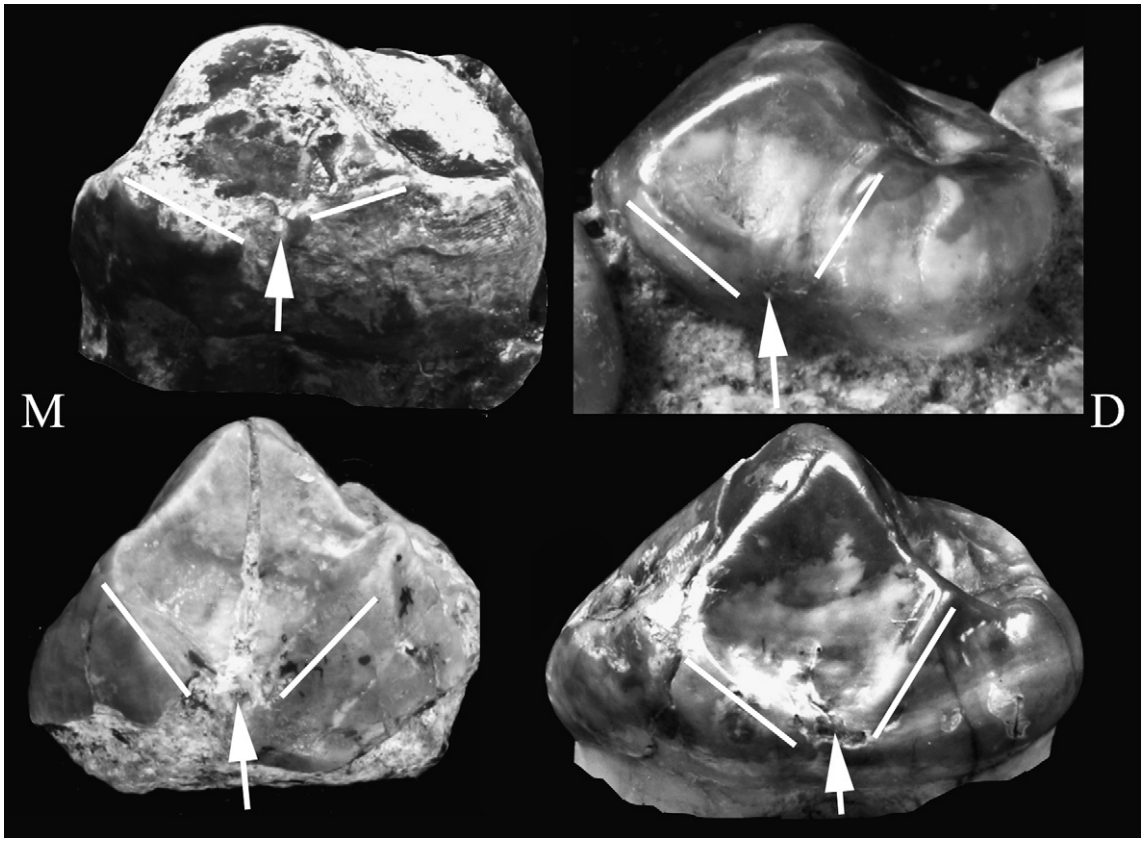

Figure 13. Lingual view of the Fa of *A. anamensis*. For all teeth, mesial (M) is to the left and distal (D) is to the right. Clockwise from the top left: KNM-ER 20432 (image reversed), KNM-KP 29281, KNM-KP 29286, and KNM-KP 29284. The Kanapoi specimens express a diamond-shaped Fa formed by a tall Prd, sharp steeply-angled Tc, sharp steeply-angled Mpc, and weakly-developed and steeply-sloped Mmr (the lingual and buccal segments are indicated with white lines) in which the two segments meet at an angle near the cervix of the tooth (indicated with a white arrow). The configuration observed in the Kanapoi specimens recalls the morphology observed in *P. troglodytes* (Fig. 4). Because the Mmr is more developed and does not slope inferiorly as strongly in KNM-ER 20432 as it does in the Kanapoi sample, the Fa has a flatter base. When viewed occlusally, the KNM-ER 20432 Fa appears more pit-like than in the Kanapoi sample.

feature set of the youngest sample appeared at different times (e.g., Kimbel et al., 2006). The earliest *A. anamensis* P_3s from Kanapoi express a consistent package of plesiomorphic features (large Fa Area relative to Fp Area, weakly-developed Mmr, diamond-shaped Fa, mesiolingually open Fa, sharp occlusal crests, Med absence, distolingually-oriented Tc). Departures appear in the younger *A. anamensis* P_3 from Allia Bay (slight Fp expansion, elevation of the buccal segment of the Mmr); however, the Allia Bay P_3 is unicuspid and has a broad buccal face, as in the Kanapoi sample. Additional derived features appear first in the Laetoli sample (further expansion of the Fp, variable expression of Mmr fusion, Med presence), while the crown is MD elongated relative to BL width. The variable expression of Mmr fusion and Med presence persists into the younger Ethiopian *A. afarensis* P_3s, while the Fa becomes further restricted and occasionally closed by an elevated and fused Mmr, the Fp is further expanded, the Med is more mesially shifted, and the crown becomes BL expanded relative to its MD length (especially so in the youngest, KH-2, P_3s). Thus, the pattern of character-state change within the *A. anamensis*–*A. afarensis* lineage suggests that P_3 evolution was strongly mosaic.

Not only do apomorphic features largely vary independently of one another in *A. afarensis*, they are independent of occlusal size. In the 1970s *A. afarensis* sample, two small P_3s, A.L. 288-1 and A.L. 128-23, which are unicuspid and have fairly open Fas (because they lack prominent lingual segments of the Mmr), anchored the primitive end of *A. afarensis* P_3 crown morphocline; however, A.L. 277-1 (a large unicuspid specimen) demonstrated that there is not a strong morphological association between the presence of derived features and crown size. Two specimens recently discovered at Hadar reinforce this observation. A large (presumptive male) P_3, A.L. 1496-1, expresses many plesiomorphic features (minimally-developed Med; incompletely-fused Mmr; centrally-placed Pd) and, conversely, one of the smallest *A. afarensis* P_3s, A.L. 315-22, expresses many apomorphic features (e.g., well-developed Med that is separated from the Prd by the longitudinal groove). The features of the A.L. 315-22 P_3 are easily matched in the larger A.L. 333w-1a P_3 (Fig. 6), but are lacking in other small P_3s (i.e., A.L. 128-23 and A.L. 288-1). The independence of crown size and shape is also emphasized by the recently recovered A.L. 437-2, A.L. 1515-1, and DIK-2-1 P_3s. These P_3s are among the largest known in the Ethiopian *A. afarensis* sample and differ strongly in crown shape from the largest Laetoli P_3s, which are more elongated MD (Fig. 10). Recent additions to the *A. afarensis* hypodigm cement the observation that the presence/absence of derived features is not related to occlusal size and that crown shape and size vary independently of one another.

Molarisation of the P_3

In extant catarrhines, the P_3 occludes mesiobuccally with the maxillary canine and acts as a hone (Walker, 1984) and also occludes distally with the P^3 to function as a masticatory device. The morphology of the P_3 in extant nonhuman catarrhines must

represent a balance of these functions. Reduction in canine size and changes in canine crown shape within the hominin clade eliminated honing (Greenfield, 1990), "freeing" the P_3 to devote relatively more area distally to mastication and relatively less to the mesial portion of the crown where the minimally projecting maxillary canine occludes. Previous studies have highlighted the functional-adaptive transformation of the premolars to a highly molarised form in *Australopithecus* and especially *Paranthropus* (e.g., Robinson, 1956; Grine, 1985; Wood and Uytterschaut, 1987; Suwa, 1988, 1990; Suwa et al., 1996).

In their study of Plio-Pleistocene hominin premolar crown morphology, Wood and Uytterschaut (1987: 144) refer to molarisation of the premolars in the following manner: "In the paleontological literature, 'molarised' is the term used for premolars which have a relatively large talonid, and which may, or may not, have additional cusps." They defined talonid area as the area distal to the transverse fissure and the intersecting points on the lingual and buccal borders of the tooth. In our study, the talonid area is not measured in this manner because the transverse fissure is difficult to define on *G. gorilla* P_3s. Instead, the Fp Area is considered as a proxy for talonid size as it is a feature defined by landmarks common to all hominoid P_3s. The talonid area, as defined by Wood and Uytterschaut (1987), would not extend mesially to the Tc, as does Fp Area, and it would extend buccally past the Dpc, which defines the buccal edge of the Fp. Therefore, the Relative Fp Area of this study and the relative talonid area of Wood and Uytterschaut (1987) are not directly comparable; nevertheless, if one considers the Relative Fp Area as a proxy for relative talonid size, it is clear that *A. afarensis* has the most molarised P_3 in our study. The addition of cusps is not considered in the definition of molarisation presented above; however, the presence of a well-developed Med on some *A. afarensis* P_3s—and their near ubiquity in geologically younger species of *Australopithecus* and *Paranthropus*—must represent evidence for the changing biological role of this tooth. The result of P_3 molarisation is that mandibular premolar heteromorphy is minimal in later hominins, including *Homo sapiens*.

While increasing molarisation of the P_3 is observed in early *Australopithecus*, this trend does not coincide with the development of postcanine megadontia, strictly speaking. *A. anamensis* is the geologically oldest and most basal taxon referred to *Australopithecus* but its premolar and molar crowns are megadont, thickly enameled, and similar in size to those of *A. afarensis* (Ward et al., 2001; White et al., 2006; Kimbel and Delezene, 2009; Haile-Selassie et al., 2010b). Thus, postcanine megadontia currently appears to be a synapomorphy of all australopith-grade (*Australopithecus* + *Paranthropus*) taxa. As regards mean P_3 Projected Occlusal Area, *A. anamensis* is not significantly different from Ethiopian or Laetoli *A. afarensis* (Tables 7 and 8). Assuming that the true mean of crown size in the Laetoli sample is actually smaller than what is currently observed (the taphonomic bias in the Laetoli sample has been discussed above), these means reveal that the differences in occlusal size do not match differences in P_3 molarisation observed among the sites. The retention of a plesiomorphic feature set in the Kanapoi *A. anamensis* P_3 indicates that while postcanine megadontia and P_3 molarisation may be the product of similar selective pressures related to mastication, the morphological changes occurred independently of one another.

That P_3 molarisation and megadontia appeared independently in early *Australopithecus* suggests possible explanations for the appearances of these characteristics. Perhaps P_3 crown size was not the target of selection and the increase in its crown size represents a pleiotropic effect of selection on the other postcanine teeth. That is, as the P_4 and molar crowns increased in size in response to selection, the P_3 correspondingly increased. Perhaps size and occlusal form solve two different functional problems. To distinguish these alternatives, it will be necessary to determine the extent to which the early *Australopithecus* P_3 was used functionally like the P_4 and molars. To this end, studies of patterns of macro- and microwear on *Australopithecus* premolars would be informative.

Presumably, the expansion of the Fp and the talonid of the mandibular premolars during hominin evolution is an adaptation to changing masticatory demands. As *Paranthropus* premolars are the largest and also have the most expanded talonids, the hypothesis that premolar molarisation is an allometric effect of increasing crown size must also be considered (e.g., Wood and Uytterschaut, 1987; Suwa, 1990). Neither Suwa (1990) nor Wood and Uytterschaut (1987) found evidence for an allometric link between P_3 premolar crown size and talonid expansion among "gracile" *Australopithecus* specimens. In the current study, although KT 12/H1, DIK-2-1, and KNM-WT 8556 all fall towards the upper end of Projected Occlusal Area and Relative Fp Area, the correlation between Relative Fp Area and Projected Occlusal Area is nonsignificant when only hominin specimens are considered ($R^2 = 0.073$; $p = 0.71$) and when all hominoids are pooled ($R^2 = 0.0016$; $p = 0.72$). Moreover, if an allometric relationship between crown size and molarisation existed, then we would expect *G. gorilla* to have a larger Relative Fp Area than the hominins, which is not the case. These results reinforce the findings of Wood and Uytterschaut (1987) and Suwa (1990), which indicated that allometry does not explain the expansion of the distal portion of the hominin P_3 crown.

P_3 crown variation and hominin lineage diversity at 3.0–4.0 Ma

A. afarensis is best represented at Hadar and Laetoli, but is also documented at Maka (3.4 Ma) (White et al., 1993, 2000) and Dikika, Ethiopia (≥3.4 Ma) (Alemseged et al., 2005, 2006), the Turkana Basin of Kenya (ca. 3.3 Ma) (Kimbel, 1988; Brown et al., 2001), and possibly in the Usno Formation, Ethiopia (3.05 Ma) and Koro Toro, Chad (ca. 3.0–3.5 Ma) (Suwa, 1990; Brunet et al., 1995, 1996; Lebatard et al., 2008). The hominin remains from Dikika and Maka are referred with confidence to *A. afarensis* (White et al., 2000; Alemseged et al., 2005) and this study confirms the similarity of their P_3 morphology to paradigmatic examples from Hadar and Laetoli. The Dikika P_3, DIK-2-1, is truly remarkable among *A. afarensis* specimens for its large size, but it is like Hadar P_3s in crown shape and occlusal form (Alemseged et al., 2005).

Relative to *A. anamensis*, the P_3 crown of the *A. bahrelghazali* holotype, KT 12/H1, shares synapomorphies with *A. afarensis* (presence of well-developed Med, rounded crests, reduced Fa, expanded Fp, BL-broad crown relative to MD length) and lies outside the *A. afarensis* range of variation only in a single character considered in this study (Distal Crown Breadth/Midcrown Breadth). In fact, on the PCA, KT 12/H1 is most similar to *A. afarensis* specimen DIK-2-1 among all specimens included in the analysis (Fig. 11). Considered as a constellation of features, the occlusal morphology of KT 12/H1 falls towards the derived end of the *A. afarensis* morphological continuum, but it is not diagnosably distinct from paradigmatic examples of *A. afarensis* (but see Guy et al. (2008) for a discussion of potentially diagnostic features in the *A. bahrelghazali* mandibular symphysis). Similarly, KNM-WT 8556 is clearly derived relative to *A. anamensis* and is similar to *A. afarensis* specimens in crown shape (it is BL broad relative to MD length), crest roundness, Fp expansion, Tc orientation, and the presence of a well-developed Med that is topographically separated from the Prd by a deeply-incised longitudinal groove. The Fa of KNM-WT 8556 faces more mesially than is typically observed in *A. afarensis* (Fig. 14); however, a similar configuration is seen in A.L. 333w-1a and A.L. 315-22 (both have well-developed Meds that are topographically separated from the Prd). The Lomekwi specimen also possesses a fairly weakly-developed Mmr and a small distolingual cuspid (Fig. 14; Brown et al.,

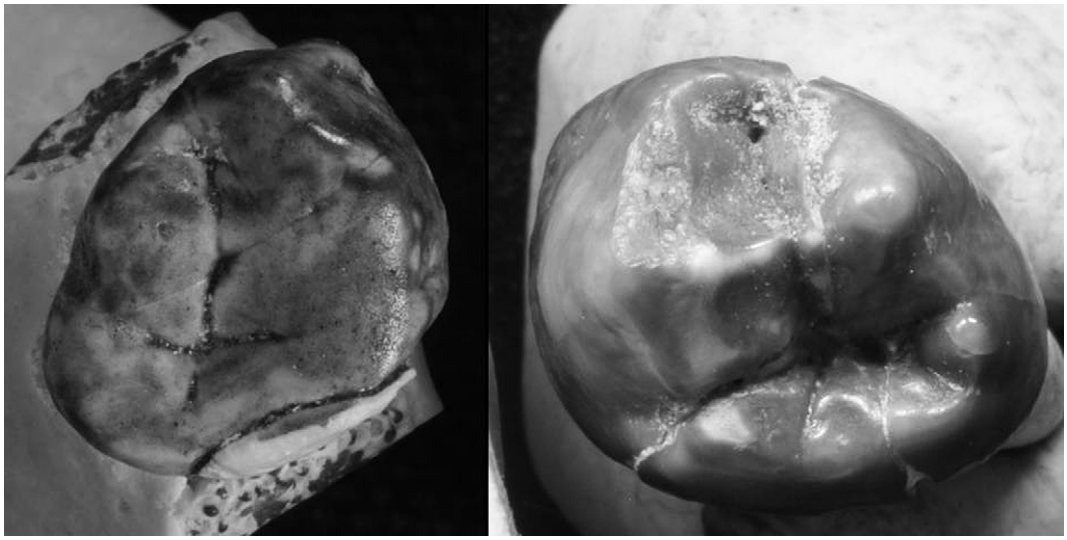

Figure 14. On left, right P_3 of KT 12/H1; on right, left P_3 of KNM-WT 8556. Photos not to scale. The KT 12/H1 P_3 differs from the typical *A. afarensis* condition in its exceptionally broad distal crown and expansive Fp. The KNM-WT 8556 P_3 differs from the typical *A. afarensis* condition in the mesially directed Fa, the poorly-developed Mmr, and the presence of a distolingual cuspid.

2001), both of which are rare in the *A. afarensis* hypodigm (Suwa, 1990). Minimal wear along the Dmr would erase the distolingual cuspid, so the frequency of this trait is at present unknown for *A. afarensis*. As with KT 12/H1, the character states present in KNM-WT 8556 place it towards the derived end of the morphological spectrum observed in *A. afarensis*; however, the range of variation observed in *A. afarensis* easily accommodates this specimen. Though descriptions of the Woranso-Mille P_3s have been limited and focused on ARI-VP-3/80, they are described as morphologically intermediate between older *A. anamensis* (Kanapoi, Allia Bay) and younger *A. afarensis* samples (Laetoli, Hadar, Maka, Dikika), which supports the hypothesis that *A. anamensis* and *A. afarensis* are ancestor and descendant taxa, respectively (Haile-Selassie, 2010; Haile-Selassie et al., 2010a,b). By themselves, neither the Koro Toro and Lomekwi P_3s, nor the Woranso-Mille P_3 sample, hint at hominin *lineage* diversity in the African middle Pliocene (see Kimbel et al. (2006) and Haile-Selassie (2010) for discussion of the taxonomic issues raised by the recognition of the *A. anamensis–A. afarensis* lineage).

Conclusions

The samples of P_3s attributed to *A. anamensis* and *A. afarensis* capture the incipient stages of the molarisation of the hominin P_3. The *A. anamensis–A. afarensis* lineage begins with a nearly homogenous, plesiomorphic feature set at Kanapoi (large Fa Area relative to Fp Area, weakly-developed Mmr, diamond-shaped Fa, mesiolingually open Fa, sharp crests, Med absence, distolingually-oriented Tc). Incipient molarisation (Fp expansion) and Fa reorganization (the elevation of the Mmr) are evident in the single known Allia Bay P_3. The Laetoli sample is characterized by a further expansion of the Fp and variable expression of derived features (Mmr fusion), but the sample retains a MD-elongated crown and some individuals retain a relatively large Fa. The variable expression of derived character states persists into the Ethiopian sample of *A. afarensis*, while crown shape changes to become more BL broad relative to MD length and the Fa becomes even further restricted and is sometimes closed. Subsequently, the variable features observed in *A. afarensis* become fixed in *Australopithecus* and *Paranthropus* (Med presence, Mmr prominence, Fa closure) and the trends towards crown shape change and P_3 molarisation continue, reaching their fullest elaboration in *Paranthropus*. Since the variable apomorphic features of *A. afarensis* are absent in more ancient taxa and then become fixed in geologically younger taxa, the evolutionary changes observed in the P_3 of the *A. anamensis–A. afarensis* lineage bridge the significant morphological gap between geologically younger hominins (i.e., *A. africanus*, *Paranthropus*, *Homo*) on the one hand, and extant apes and *Ardipithecus* on the other. The sample of P_3s attributed to *A. afarensis*, in particular, reveals the mosaic nature of the acquisition of derived P_3 crown character states. Though the P_3 morphology of *A. anamensis* differs from that of extant African apes, relative to geologically younger hominin taxa the *A. anamensis* sample (especially the Kanapoi specimens) is demonstrably plesiomorphic. The retention of plesiomorphic features in *A. anamensis* shows that a significant transition from an ape-like P_3 form to an apomorphic occlusal form does not coincide with the loss of canine honing in hominins, which is supported by the retention of a plesiomorphic P_3 in *Ar. ramidus*, in which canine honing was already lost (White et al., 1994; Semaw et al., 2005; Suwa et al., 2009). In early *Australopithecus*, the expansion of the Fp of the P_3 occurs after the loss of functional canine honing (evident in *Ar. ramidus*) and after the appearance of postcanine megadontia (evident in Asa Issie and Kanapoi *A. anamensis*). The evolution of P_3 crown morphology in *A. afarensis* and *A. anamensis* constitutes a detailed paleontological illustration of the disintegration and subsequent refashioning of a functionally integrated morphological complex to reflect an apomorphic enhancement of an existing biological role.

Acknowledgements

We thank the staff of the National Museum of Ethiopia, especially General Manager Mamitu Yilma and casting expert Alemu Ademassu, for granting access to the Hadar specimens; Dr. Emma Mbua, the staff of the National Museums of Kenya, and Dr. Meave Leakey for permission to study the *A. anamensis* and Lomekwi fossils; Lyman Jellema for providing access to and assistance with the Hamann-Todd Osteological Collection at the Cleveland Museum of Natural History; and Malcolm Harmon and the staff of the Powell-Cotton Museum for access to and assistance with their collection. We also thank Linda Gordon (Smithsonian Museum of Natural History), Bill Stanley (Field Museum of Natural History), and Eileen Westwig (American Museum of Natural History) for

permission to access their collections. We are grateful to Dr. Zeresenay Alemseged for providing a cast of DIK-2-1 and permitting us to study the original specimen, Dr. Michel Brunet for providing a cast of the P_3s of KT 12/H1 and allowing us to include data collected from this specimen, and the late Dr. Charles Lockwood for providing the Excel macros used to perform the permutation tests, bootstrapping procedures, and tests of temporal trends that were used in this analysis. We thank Dr. Matt Tocheri for helpful discussions related to statistical testing and comments on an early version of this manuscript. Comments from three anonymous reviews and those of editor Dr. Steve Leigh greatly improved the manuscript. A portion of the data analyzed here was collected as part of LKD's Masters-in-passing thesis research, which benefited from the financial support of the Research and Development Committee of the School of Human Evolution and Social Change and the Institute of Human Origins at Arizona State University. Data collection was also funded by a Wenner-Gren Doctoral Dissertation Fieldwork Grant and NSF Doctoral Dissertation Improvement Grant (# 0852105) to LKD (under WHK).

References

Alemseged, Z., Wynn, J.G., Kimbel, W.H., Reed, D., Geraads, D., Bobe, R., 2005. A new hominin from the Basal Member of the Hadar Formation, Dikika, Ethiopia and its geological context. J. Hum. Evol. 49, 499–514.

Alemseged, Z., Spoor, F., Kimbel, W.H., Bobe, R., Geraads, D., Reed, D., Wynn, J.G., 2006. A juvenile early hominin skeleton from Dikika, Ethiopia. Nature 443, 296–301.

Bailey, S.E., Lynch, J.M., 2005. Diagnostic differences in mandibular P4 shape between Neandertals and anatomically modern humans. Am. J. Phys. Anthropol. 126, 268–277.

Bailey, S.E., Wood, B.A., 2007. Trends in postcanine occlusal morphology within the hominin clade: the case of *Paranthropus*. In: Bailey, S.E., Hublin, J.-J. (Eds.), Dental Perspectives on Human Evolution: State-of-the-Art Research in Dental Paleoanthropology. Springer, New York, pp. 33–52.

Brown, B., Brown, F.H., Walker, A., 2001. New hominids from the Lake Turkana basin, Kenya. J. Hum. Evol. 41, 29–44.

Brunet, M., Beauvilain, A., Coppens, Y., Heintz, E., Moutaye, A.H.E., Pilbeam, D., 1995. The first australopithecine 2,500 kilometres west of the Rift Valley (Chad). Nature 378, 273–275.

Brunet, M., Beauvilain, A., Coppens, Y., Heintz, E., Moutaye, A.H.E., Pilbeam, D., 1996. *Australopithecus bahrelghazali*, une nouvelle espece d'Hominide ancient de la region de Koro Toro (Tchad). C.R. Acad. Sci. 322, 907–913.

Brunet, M., Guy, F., Pilbeam, D., Mackaye, H.T., Likius, A., Ahounta, D., Beauvilain, A., Blondel, C., Bocherens, H., Boisserie, J.R., De Bonis, L., Coppens, Y., Dejax, J., Denys, C., Duringer, P., Eisenmann, V.R., Fanone, G., Fronty, P., Geraads, D., Lehmann, T., Lihoreau, F., Louchart, A., Mahamat, A., Merceron, G., Mouchelin, G., Otero, O., Campomanes, P.P., Ponce De Leon, M., Rage, J.C., Sapanet, M., Schuster, M., Sudre, J., Tassy, P., Valentin, X., Vignaud, P., Viriot, L., Zazze, A., Zollikofer, C., 2002. A new hominid from the Upper Miocene of Chad, Central Africa. Nature 418, 145–151.

Campisano, C.J., Feibel, C.S., 2008. Depositional environments and stratigraphic summary of the Pliocene Hadar Formation at Hadar, Afar Depression, Ethiopia. GSA Special Papers 446, 179–201.

Coppens, Y., 1977. Evolution morphologique de la premie`re premolaireinférieure chez certains Primates supérieurs. C.R. Acad. Sci. D 285, 1299–1302.

Deino, A.L., Scott, G.R., Saylor, B., Alene, M., Angelini, J.D., Haile-Selassie, Y., 2010. $^{40}Ar/^{39}Ar$ datin, paleomagnetism, and tephrochemistry of Pliocene strata of the hominid-bearing Woranso-Mille area, west-central Afar Rift, Ethiopia. J. Hum. Evol. 58, 111–126.

Garcia, L.V., 2004. Escaping the Bonferroni iron claw in ecological studies. Oikos 105, 657–663.

Greenfield, L.O., 1990. Canine "honing" in *Australopithecus afarensis*. Am. J. Phys. Anthropol. 82, 135–143.

Greenfield, L.O., Washburn, A., 1992. Polymorphic aspects of male anthropoid honing premolars. Am. J. Phys. Anthropol. 87, 173–186.

Grine, F.E., 1985. Australopithecine evolution: the deciduous dental evidence. In: Delson, E. (Ed.), Ancestors: The Hard Evidence. Alan R. Liss, New York, pp. 153–167.

Guy, F., Mackaye, H.T., Likius, A., Vignaud, P., Schmittbuhl, M., Brunet, M., 2008. Symphyseal shape variation in extant and fossil hominoids, and the symphysis of *Australopithecus bahrelghazali*. J. Hum. Evol. 55, 37–47.

Haile-Selassie, Y., 2001. Late Miocene hominids from the Middle Awash, Ethiopia. Nature 412, 178–181.

Haile-Selassie, Y., 2010. Phylogeny of early *Australopithecus*: new fossil evidence from the Woranso-Mille (central Afar, Ethiopia). Philos. Tran. R. Soc. Lond. B. 365, 3323–3331.

Haile-Selassie, Y., Latimer, B.M., Alene, M., Deino, A.L., Gibert, L., Melillo, S.E., Saylor, B.Z., Scott, G.R., Lovejoy, C.O., 2010a. An early *Australopithecus afarensis* postcranium from Woranso-Mille, Ethiopia. Proc. Natl. Acad. Sci. USA 107, 12121–12126.

Haile-Selassie, Y., Saylor, B.Z., Deino, A., Alene, M., Latimer, B.M., 2010b. New hominid fossils from Woranso-Mille. Am. J. Phys. Anthropol. 141, 406–417.

Haile-Selassie, Y., Suwa, G., White, T.D., 2004. Late Miocene teeth from Middle Awash, Ethiopia, and early hominid dental evolution. Science 303, 1503–1505.

Haile-Selassie, Y., Suwa, G., White, T.D., 2009. Hominidae. In: Haile-Selassie, Y., WoldeGabriel, G. (Eds.), *Ardipithecus kadabba*: Late Miocene Evidence from the Middle Awash, Ethiopia. University of California Press, Berkeley, pp. 159–236.

Johanson, D.C., White, T.D., Coppens, Y., 1982. Dental remains from the Hadar formation, Ethiopia, 1974–1977 collections. Am. J. Phys. Anthropol. 57, 545–603.

Johnson, R.A., Wichern, D.W., 2007. Applied Multivariate Statistical Analysis, sixth ed. Prentice-Hall, Upper Saddle River, NJ.

Kimbel, W.H., 1988. Identification of a partial cranium of *Australopithecus afarensis* from the Koobi Fora Formation, Kenya. J. Hum. Evol. 17, 647–656.

Kimbel, W.H., Delezene, L.K., 2009. Lucy "Redux" a review of research on *Australopithecus afarensis*. Yearb. Phys. Anthropol. 52, 2–48.

Kimbel, W.H., Rak, Y., Johanson, D.C., 2004. The Skull of *Australopithecus afarensis*. Oxford University Press, New York.

Kimbel, W.H., Lockwood, C.A., Ward, C.V., Leakey, M.G., Rak, Y., Johanson, D.C., 2006. Was *Australopithecus anamensis* ancestral to *A. afarensis*? A case of anagensis in the hominin fossil record. J. Hum. Evol. 51, 565–571.

Kimbel, W.H., White, T.D., Johanson, D.C., 1985. Craniodental morphology of the hominids from Hadar and Laetoli: evidence of "*Paranthropus*" and *Homo* in the Mid-Pliocene of eastern Africa. In: Delson, E. (Ed.), Ancestors: The Hard Evidence. Liss, New York, pp. 120–137.

Kinzey, W.G., 1971. Evolution of the human canine tooth. Am. Athropol. 73, 680–694.

Leakey, M.G., Feibel, C.S., McDougall, I., Walker, A., 1995. New four-million-year-old hominid species from Kanapoi and Allia Bay, Kenya. Nature 376, 565–571.

Leakey, M.G., Feibel, C.S., McDougall, I., Ward, C., Walker, A., 1998. New specimens and confirmation of an early age for *Australopithecus anamensis*. Nature 393, 62–66.

Leakey, M.G., Spoor, F., Brown, F.H., Gathogo, P.N., Kiarie, C., Leakey, L.N., McDougall, I., 2001. New hominin genus from eastern Africa shows diverse middle Pliocene lineages. Nature 410, 433–440.

Lebatard, A.E., Bourlès, D.L., Duringer, P., Jolivet, M., Braucher, R., Carcaillet, J., Schuster, M., Arnaud, N., Monié, P., Hihoreau, F., Likius, A., Mackaye, H.T., Vignaud, P., Brunet, M., 2008. Cosmogenic nuclide dating of *Sahelanthropus tchadensis* and *Australopithecus bahrelghazali*: Mio-Pliocene hominids from Chad. Proc. Natl. Acad. Sci. USA 105, 3226–3231.

Leonard, W.R., Hegmon, M., 1987. Evolution of P_3 morphology in *Australopithecus afarensis*. Am. J. Phys. Anthropol. 73, 41–63.

Lockwood, C.A., Kimbel, W.H., Johanson, D.C., 2000. Temporal trends and metric variation in the mandibles and dentition of *Australopithecus afarensis*. J. Hum. Evol. 39, 23–55.

Manly, B.F.J., 2001. Randomization, Bootstrap and Monte Carlo Methods in Biology, second ed. Chapman and Hall, CRC, Baco Raton, Florida.

Moran, M.D., 2003. Arguments for rejecting the sequential Bonferroni in ecological studies. Oikos 100, 403–405.

Nakagawa, S., 2004. A farewell to Bonferroni: the problems of low statistical power and publication bias. Behav. Ecol. 15, 1044–1045.

Olson, T.R., 1985. Cranial morphology and systematics of the Hadar Formation hominids and "*Australopithecus*" *africanus*. In: Delson, E. (Ed.), Ancestors: The Hard Evidence. Liss, New York, pp. 102–119.

Remis, M.J., 2006. The role of taste in food selection by African apes: Implications for niche separation and overlap in tropical forests. Primates 47, 56–64.

Robinson, J.T., 1956. The dentition of the Australopithecinae. Memoir No. 9. Transvaal Museum. South Africa, Pretoria.

Roman, D.C., Campisano, C.J., Quade, J., DiMaggio, E., Arrowsmith, J.R., Feibel, C., 2008. Composite tephrostratigraphy of the Dikika, Gona, Hadar, and Ledi-Geraru project areas, northern Awash, Ethiopia. GSA Special Papers 446, 119–134.

Ryan, A.S., Johanson, D.C., 1989. Anterior dental microwear in *Australopithecus afarensis*. J. Hum. Evol. 18, 235–268.

Semaw, S., Simpson, S.W., Quade, J., Renne, P.R., Butler, R.F., McIntosh, W.C., Levin, N., Dominguez-Rodrigo, M., Rogers, M.J., 2005. Early Pliocene hominids from Gona, Ethiopia. Nature 433, 301–305.

Senut, B., Pickford, M., Gommery, D., Mein, P., Cheboi, K., Coppens, Y., 2001. First hominid from the Miocene (Lukeino Formation, Kenya). C.R. Acad. Sci. Paris, Earth Planet. Sci. 332, 137–144.

Simpson, S.W., Quade, J., Kleinsasser, L., Levin, N., MacIntosh, W., Dunbars, N., Semaw, S., 2007. Late Miocene hominid teeth from Gona project area, Ethiopia. Am. J. Phys. Anthropol. S44, 219.

Stanford, C.B., Nkurunungi, J.B., 2003. Behavioral ecology of sympatric chimpanzees and gorillas in Bwindi Impenetrable National Park, Uganda: diet. Int. J. Primatol. 24, 901–918.

StatSoft, Inc., 2005. STATISTICA (Data Analysis Software System), Version 7.1. www.statsoft.com.

Suwa, G., 1988. Evolution of the "robust" australopithecines in the Omo succession, evidence from mandibular premolar morphology. In: Grine, F.E. (Ed.), Evolutionary History of the "Robust" Australopithecines. Aldine de Gruyter, New York, pp. 199–222.

Suwa, G., 1990. A comparative analysis of hominid dental remains from the Shungura and Usno Formations, Omo valley, Ethiopia. University of California, Berkeley.
Suwa, G., White, T.D., Howell, F.C., 1996. Mandibular postcanine dentition from the Shungura formation, Ethiopia, crown morphology, taxonomic allocations, and Plio-Pleistocene hominid evolution. Am. J. Phys. Anthropol. 101, 247–282.
Suwa, G., Kono, R.T., Simpson, S.W., Asfaw, B., Lovejoy, C.O., White, T.D., 2009. Paleobiological implications of the *Ardipithecus ramidus* dentition. Science 326, 94–99.
Taylor, A.B., 2006. Diet and mandibular morphology in African apes. Int. J. Primatol. 27, 181–201.
Todman, J.B., Dugard, P., 2001. Single-Case and Small-*n* Experimental Designs, a Practical Guide to Randomization Tests. Lawrence Erlbaum Associates, Inc., Mahway, NJ.
Walker, A., 1984. Mechanisms of honing in the male baboon canine. Am. J. Phys. Anthropol. 65, 47–60.
Ward, C.V., Leakey, M.G., Walker, A., 1999. The new hominid species *Australopithecus anamensis*. Evol. Anthropol. 7, 197–205.
Ward, C.V., Leakey, M.G., Walker, A., 2001. Morphology of *Australopithecus anamensis* from Kanapoi and Allia Bay, Kenya. J. Hum. Evol. 41, 255–368.
White, T.D., 1977. New fossil hominids from Laetolil, Tanzania. Am. J. Phys. Anthropol. 46, 197–230.
White, T.D., 1980. Additional fossil hominids from Laetoli, Tanzania: 1976–1979 specimens. Am. J. Phys. Anthropol. 53, 487–504.
White, T.D., 1985. The hominids of Hadar and Laetoli: an element-by-element comparison of the dental samples. In: Delson, E. (Ed.), Ancestors: The Hard Evidence. Liss, New York, pp. 138–152.
White, T.D., Suwa, G., Hart, W.K., Walter, R.C., WoldeGabriel, G., Deheinzelin, J., Clark, J.D., Asfaw, B., Vrba, E., 1993. New discoveries of *Australopithecus* at Maka in Ethiopia. Nature 366, 261–265.
White, T.D., Suwa, G., Asfaw, B., 1994. *Australopithecus ramidus*, a new species of early hominid from Aramis, Ethiopia. Nature 371, 306–312.
White, T.D., Suwa, G., Simpson, S., Asfaw, B., 2000. Jaws and teeth of *Australopithecus afarensis* from Maka, Middle Awash, Ethiopia. Am. J. Phys. Anthropol. 111, 45–68.
White, T.D., WoldeGabriel, G., Asfaw, B., 2006. Asa Issie, Aramis and the origin of *Australopithecus*. Nature 440, 883–889.
Wood, B.A., Abbott, S.A., 1983. Mandibular molars, crown area measurements and morphological traits. J. Anat. 136, 197–219.
Wood, B.A., Uytterschaut, H., 1987. Analysis of the dental morphology of Plio-Pleistocene hominids. III. Mandibular premolar crowns. J. Anat. 154, 121–156.
Yamagiwa, J., Basabose, A.K., 2006. Diet and seasonal changes in sympatric gorillas and chimpanzees at Kahuzi–Biega National Park. Primates 47, 74–90.